

# Arbitrary Polynomial Separations in Trainable Quantum Machine Learning

Eric R. Anschuetz\*<sup>1</sup> and Xun Gao<sup>2</sup>

<sup>1</sup>Institute for Quantum Information and Matter, Caltech, CA, USA

<sup>1</sup>Walter Burke Institute for Theoretical Physics, Caltech, CA, USA

<sup>1</sup>MIT Center for Theoretical Physics, Cambridge, MA, USA

<sup>2</sup>JILA and Department of Physics, CU Boulder, Boulder, CO, USA

## Abstract

Recent theoretical results in quantum machine learning have demonstrated a general trade-off between the expressive power of quantum neural networks (QNNs) and their trainability; as a corollary of these results, practical exponential separations in expressive power over classical machine learning models are believed to be infeasible as such QNNs take a time to train that is exponential in the model size. We here circumvent these negative results by constructing a hierarchy of efficiently trainable QNNs that exhibit unconditionally provable, polynomial memory separations of arbitrary constant degree over classical neural networks in performing a classical sequence modeling task. Furthermore, each unit cell of the introduced class of QNNs is computationally efficient, implementable in constant time on a quantum device. The classical networks we prove a separation over include well-known examples such as recurrent neural networks and Transformers. We show that quantum contextuality is the source of the expressivity separation, suggesting that other classical sequence learning problems with long-time correlations may be a regime where practical advantages in quantum machine learning may exist.

Perdomo-Ortiz et al., 2018; Lloyd & Weedbrook, 2018; Schuld & Killoran, 2019; Havlíček et al., 2019; Killoran et al., 2019). These *quantum machine learning* (QML) models are motivated by the ability of quantum systems to naturally represent complex probability distributions that are believed to be difficult to represent classically (Gao et al., 2018; Coyle et al., 2020; Du et al., 2020; Sweke et al., 2021). Recent theoretical analysis of QML algorithms has determined that, indeed, there exist classical learning tasks that are more efficiently performed by quantum machine learning models than classical machine learning models (Gao et al., 2018; Coyle et al., 2020; Du et al., 2020; Sweke et al., 2021; Liu et al., 2021). Essentially all of these studies rely on reducing machine learning tasks to problems like factoring which are believed to be classically hard to perform yet are known to be (asymptotically) easy using quantum devices.

One of the miracles of classical machine learning is that the optimization of the extremely complicated, nonconvex loss functions that underlie all large-scale learning algorithms for neural networks is efficient. This phenomenon has only recently been understood theoretically (Choromanska et al., 2015; Chaudhari, 2018). Unfortunately, it is now known that these results do not port over to the quantum setting; generally, the training of QML models is difficult (McClean et al., 2018; Cerezo et al., 2021; Napp, 2022; Cerezo & Coles, 2021; Arrasmith et al., 2021; Anschuetz, 2022; Anschuetz & Kiani, 2022). This line of research in the quantum setting has culminated in the demonstration of a *trainability-expressivity trade-off* in quantum machine learning (Holmes et al., 2022). Effectively, this is a statement that quantum models that are exponentially more expressive than classical

## 1 Introduction

### 1.1 Motivation

In recent years the prospect of using quantum devices to aid (or fully supplant) classical devices in machine learning tasks has garnered much study (Schuld et al., 2015; Biamonte et al., 2017; Amin et al., 2018;

\*eans@caltech.edu

models are *not* efficiently trainable. This suggests that the superpolynomial separations that rely on reductions to classically hard decision problems may be optimistic as they implicitly require one to have *a priori* knowledge of what the problem is to avoid optimizing a quantum model over an exponentially large Hilbert space.

One way to sidestep these issues is by considering *restricted QML models*. Namely, one can restrict the search space over quantum models to guarantee efficient trainability. This has been recently studied in the context of symmetry-equivariant models, which use symmetries to explicitly restrict the allowed operations of the quantum model (Nguyen et al., 2022; Larocca et al., 2022b; Ragone et al., 2022). However, recent results on the efficient classical simulability of certain symmetry-equivariant models have made it unclear what symmetries exist that are restrictive enough to allow for efficient trainability, while being unrestrictive enough that a quantum advantage is maintained (Anschuetz et al., 2022; Cerezo et al., 2023).

A different approach was taken in work by Anschuetz et al. (2023), where Gaussian circuits applied to fixed non-Gaussian states were used for the basis of a QML model. There, both efficient trainability (by the results of Larocca et al. (2022a; 2023), Rudolph et al. (2023), Fontana et al. (2023), and Ragone et al. (2023)) and an expressivity separation over classical neural networks were shown. Excitingly, this separation was proved to hold (on a certain sequence modeling task) even over state-of-the-art classical models such as Transformers (Vaswani et al., 2017) including, e.g., GPT-4 (OpenAI, 2023). However, this expressivity separation was only quadratic, making an experimental implementation showcasing an advantage impractical due to the large constant overhead of quantum error correction (Babbush et al., 2021). Another drawback of this approach was that results were only known for continuous-variable (CV) quantum systems, making any experimental demonstration unsuitable for qubit-based quantum architectures due to large constant-factor overheads.

## 1.2 Our Contributions

We here for the first time balance considerations of trainability and expressivity to construct a hierarchy of trainable quantum neural networks (QNNs) that exhibit *arbitrarily large* polynomial expressivity separations over classical artificial neural networks (ANNs). Namely, we show that there exists a hi-

erarchy of sequence modeling tasks indexed by  $n, k$  that can be performed to zero error by an efficiently trainable QNN with  $O(n)$  quantum neurons. We then show that no ANN with fewer than  $\binom{n}{k} - 1$  neurons can perform this task to *any* finite cross entropy. Importantly, the ANNs we prove a memory separation against includes state-of-the-art models like GPT-4 (OpenAI, 2023). We construct hierarchies of QNNs capable of completing the task in both a CV setting as well as a qubit setting. Our results can also be viewed as a quantum-classical communication separation in performing a certain sampling task. Viewed through this lens, our results differ from previously known quantum-classical communication complexity separations (Raz, 1999; Buhrman et al., 2001; Le Gall, 2006; Gavinsky et al., 2007; Gupta et al., 2023; Kallaughner et al., 2023; Manna et al., 2024) not only in the strength of the error model we consider, but also as our resulting model is computationally efficient when  $k$  is constant—we demonstrate that every unit cell of the recurrent QNNs we describe is in  $\text{QNC}_{\text{wf}}^0$ , i.e., every unit cell can be implemented in constant depth on a quantum computer assuming access to quantum fan-out (or logarithmic depth if not) (Moore & Nilsson, 2001; 1998; Høyer & Špalek, 2005). This can be strengthened further to constant-sized circuits (even without fan-out) at the expense of requiring longer sequence lengths or by considering an online version of the task.

We achieve this by considering QNNs that are composed of operations that climb the *Clifford hierarchy* (Gottesman & Chuang, 1999)—inductively defined as the normalizer of the previous level, with the first level the group of displacement operators—in a controlled way; our results therefore also imply memory lower-bounds for classically simulating the Clifford hierarchy through any given level. Our proof strategy involves demonstrating that certain classes of operators in this hierarchy are highly *contextual* in the sense that there exists many subsets of them from which one can construct so-called antidistinguishing measurement sequences (Leifer, 2014) via pseudo-telepathy game-like arguments (Mermin, 1990). Our result is thus also *interpretable*, as we directly demonstrate that the quantum advantage arises from the natural ability of a quantum memory to store long-time correlations more space-efficiently than a classical memory due to quantum contextuality. Though our result is proven on constructed data, this suggests sequential data with long-time correlations is a natural use-case for our introduced class of QNNs. This is similar in

spirit to the results of Anschuetz et al. (2023), where an interpretable, provable quantum advantage on a constructed translation task was shown empirically to persist when performing real-world translation tasks.

## 2 Preliminaries

### 2.1 Quantum Generative Models

A quantum system of size  $n$  is naturally represented by a *quantum state*, which is a normalized vector  $|\psi\rangle \in \mathbb{C}^N$ . Here, we use the typical physics notation  $|\cdot\rangle$  to denote a vector, instead of (say)  $\psi$ , when we are describing a quantum state, and  $\langle\psi| = |\psi\rangle^\dagger$ . Given a quantum state there is a natural induced probability distribution given by the *measurement distribution*:

$$p(x_1, \dots, x_n) = \langle\psi| \Pi_{x_1} \dots \Pi_{x_n} |\psi\rangle, \quad (1)$$

where  $\Pi_{x_i}$  are Hermitian projectors (assumed here to commute) which satisfy:

$$I_N = \sum_{x_1, \dots, x_n} \Pi_{x_1} \dots \Pi_{x_n}, \quad (2)$$

where  $I_N$  is the  $N \times N$  identity operator. If the states  $|\psi\rangle$  are optimized over such that  $p$  approximates some data distribution  $p_{\text{data}}$ , this defines a *quantum generative model*. Throughout we will often reference the Pauli operators:

$$X = \begin{pmatrix} 0 & 1 \\ 1 & 0 \end{pmatrix}, \quad Z = \begin{pmatrix} 1 & 0 \\ 0 & -1 \end{pmatrix}, \quad (3)$$

with subscript  $P_i$  shorthand for the tensor product  $I_2 \otimes \dots \otimes P \otimes \dots \otimes I_2$  for Pauli operator  $P$  at the  $i$ th position. We will also consider the canonical position and momentum operators  $\hat{q}_i, \hat{p}_i$  formally acting on an infinite-dimensional Hilbert space and obeying the so-called canonical commutation relation (in units where  $\hbar = 1/2$ ):

$$[\hat{q}_j, \hat{p}_k] = \frac{i}{2} \delta_{jk}. \quad (4)$$

For more background on quantum computation—including details of quantum circuit diagrams, as used in Figure 2—we recommend the seminal textbook of Nielsen & Chuang (2010).

### 2.2 Neural Sequence Learning

*Sequence-to-sequence* or *sequence* learning (Sutskever et al., 2014) is the approximation of some given conditional distribution  $p(\mathbf{y} | \mathbf{x})$  with a model distribution  $q(\mathbf{y} | \mathbf{x})$ , where the vectors  $\mathbf{x}, \mathbf{y}$  are tokenized

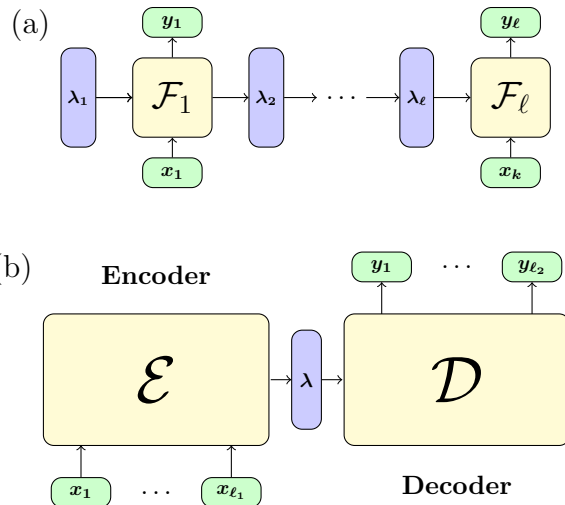


Figure 1: (a) An autoregressive neural sequence model. The model autoregressively takes input tokens  $\mathbf{x}_i$ , and outputs decoded tokens  $\mathbf{y}_i$ , with map  $\mathcal{F}_i$ . The model also has an unobserved internal memory with state  $\lambda_i \in L$  after decoding the token  $\mathbf{x}_{i-1}$  that  $\mathcal{F}_i$  can depend on. (b) A general encoder-decoder model.  $\mathcal{E}$  encodes the input  $\mathbf{x}$  into some latent representation  $\lambda \in L$ . A decoder  $\mathcal{D}$  then outputs the decoded sequence  $\mathbf{y}$ .

sequences  $(x_1, \dots, x_{l_1}), (y_1, \dots, y_{l_2})$ . This framework encompasses sentence translation tasks (Sutskever et al., 2014), speech recognition (Prabhavalkar et al., 2017), image captioning (Vinyals et al., 2015), and many more practical problems.

Sequence modeling today is typically performed using *neural sequence models*. Generally, these models are parameterized functions that take as input the sequence  $\mathbf{x}$  and output a sample from the conditional distribution  $q(\mathbf{y} | \mathbf{x})$ . The parameters of these functions are trained to minimize an appropriate loss function, such as the (forward) empirical cross entropy:

$$\hat{H}(p, q) = -\frac{1}{|\mathcal{T}|} \sum_{(\mathbf{x}, \mathbf{y}) \in \mathcal{T}} p(\mathbf{y} | \mathbf{x}) \log(q(\mathbf{y} | \mathbf{x})), \quad (5)$$

where  $\mathcal{T} = \{(\mathbf{x}_i, \mathbf{y}_i)\}$  are samples from  $p(\mathbf{x}, \mathbf{y})$ . The backward empirical cross entropy is similarly defined, with  $p \leftrightarrow q$ . Note that a model with support on an incorrect “translation” (i.e.,  $q \neq 0, p = 0$ ) yields an infinite backward cross entropy.

One of the unique challenges when performing sequence modeling is the potentially large variance in the

data dimension due to sequences of different lengths being present in the data set. Thus, to maintain a resource scaling independent of the input sequence length, neural sequence models usually fall into one of two classes: *autoregressive sequence models* (Hopfield, 1982; Hochreiter & Schmidhuber, 1997; Cho et al., 2014) or *encoder-decoder models* (Sutskever et al., 2014; Vaswani et al., 2017).

Autoregressive sequence models include traditional neural sequence models such as vanilla recurrent neural networks (RNNs) (Hopfield, 1982), long-short term memory networks (LSTMs) (Hochreiter & Schmidhuber, 1997), and gated recurrent units (GRUs) (Cho et al., 2014). Autoregressive models also include less traditional sequence models such as GPT-4 (OpenAI, 2023), which is composed solely of the autoregressive decoder of a Transformer. In autoregressive models, input tokens  $\mathbf{x}_i$  are translated in sequence to output tokens  $\mathbf{y}_i$  via functions  $\mathcal{F}_i$  (typically assumed to be identical, though we make no such requirement here). An unobserved internal memory (or *latent space*)  $L$  shared between time steps allows the model to represent long-range correlations in the data. A diagram of the general form of autoregressive models is given in Figure 1(a).

Encoder-decoder models include seq2seq models (Sutskever et al., 2014) and traditional Transformers (Vaswani et al., 2017). In encoder-decoder models, an encoder  $\mathcal{E}$  maps the input sequence  $\mathbf{x}$  to a latent space representation  $\boldsymbol{\lambda} \in L$ ; then, a decoder  $\mathcal{D}$  transforms this representation to the output sentence  $\mathbf{y}$ . The advantage of encoder-decoder models over generic representations of  $p(\mathbf{y} | \mathbf{x})$  is the improved time complexity when considering a lower dimensional representation  $\boldsymbol{\lambda}$  of  $\mathbf{x}$ . When the encoder map is trivial (i.e., when  $L$  is congruent to the input space and  $\mathcal{E}$  is the identity), then no compression occurs, and the model is equivalent to a general representation of  $p(\mathbf{y} | \mathbf{x})$  given by  $\mathcal{D}$ . A diagram of the general form of encoder-decoder models is given in Figure 1(b).

We have not yet stated any requirements on the model functions  $\mathcal{F}_i$  (or  $\mathcal{E}, \mathcal{D}$ ). If these functions were allowed to be fully general, they could in principle implement arbitrarily complicated functions. In practice, however, training over extremely large model spaces is inefficient, and typically  $\mathcal{F}_i(\mathcal{E}, \mathcal{D})$  are composed of functions with some sort of smoothness structure. Thus, in the following, we effectively assume two properties of classical neural networks (for a detailed account of our assumptions, see Appendix C):

**Assumption 2.1** ( $C^2$  model on finite volume sub-

space).  $\mathcal{F}_i(\mathcal{E})$  is continuously second-differentiable on a finite-measure subspace of inputs;

**Assumption 2.2** (Strong submersion on finite volume subspace).  $\mathcal{F}_i(\mathcal{E})$  is a *strong submersion* on this subspace of inputs.

We make no assumptions on the form of the decoder  $\mathcal{D}$ .

Assumption 2.1 is straightforward and is automatically satisfied by models composed of linear layers along with rectified linear units, softmax functions, sigmoid functions, hyperbolic tangent functions, and other standard nonlinearities. Assumption 2.2 is slightly more subtle, and is a requirement that there exists a finite volume subspace of the inputs where the Jacobian of the model is of maximal rank (with associated minor having lower-bounded determinant). Stated another way, we require that there is a finite volume subspace of the inputs that are not near-critical points of  $\mathcal{F}_i(\mathcal{E})$ . This is effectively a requirement that the model is *strongly Morse* (Mokhtari et al., 2019) in a multivariate sense. Neural networks being strongly Morse (in the univariate sense) is a common assumption (Mei et al., 2018; Mokhtari et al., 2019; Yang et al., 2021; Dixit et al., 2023), and certain classes of neural networks are known to be almost surely Morse over settings of their parameters (Kurochkin, 2021). In Appendix C we give natural settings where these Assumptions are automatically satisfied and also discuss an additional minor technical assumption on the latent space  $L$  used in the proofs of our theorems.

## 2.3 Efficient Trainability From Bounded Dynamical Lie Algebra Dimension

To demonstrate the trainability of our introduced class of QNNs we will bound the dimension of the *dynamical Lie algebra* (Larocca et al., 2022a; 2023) associated with the model. As we will later see, our class of models can be described as a parameterized class of quantum states:

$$|\boldsymbol{\theta} | \mathbf{x}\rangle \equiv \prod_{i=1}^p \exp(-i\theta_i \hat{Q}_i) |\psi_0(\mathbf{x})\rangle \quad (6)$$

for certain Hermitian operators  $\hat{Q}_i$ , where here  $|\psi_0(\mathbf{x})\rangle$  is a computational basis state or Gaussian state dependent on the input  $\mathbf{x}$ , and the output of the model is given by expectation values of local observables in this state. We assume there exists a natural

scaling of  $|\boldsymbol{\theta} | \boldsymbol{x}\rangle$  with the model size  $n$ , as we have here. The dynamical Lie algebra  $\mathfrak{g}$  associated with a model of this form is given by the Lie algebra generated by the generators  $\hat{Q}_i$  (Larocca et al., 2022a; 2023), i.e.,

$$\mathfrak{g} = \text{span} \left\langle \left\{ i\hat{Q}_i \right\}_{i=1}^p \right\rangle_{\text{Lie}}. \quad (7)$$

In the work of Larocca et al. (2023) it was conjectured—and later proven by the work of Fontana et al. (2023) and Ragone et al. (2023)—that the variance of gradients over the loss landscape of such QNNs scale *inverse polynomially* in the dimension of  $\mathfrak{g}$ . Furthermore, evidence was given that when  $\dim(\mathfrak{g})$  scales polynomially in  $n$  it is easy to reach an *overparameterized phase* where the local minima of the associated loss function are close in function value to the global minimum. Efficient trainability of such models using loss functions more typical for generative modeling—such as the maximum mean discrepancy (MMD) loss—was further conjectured and given evidence for in the work of Rudolph et al. (2023). In Section 3 we will discuss the dynamical Lie algebra of the models we here introduce in detail and indeed show polynomial scaling of its dimension with the model size for the CV version of our class of models. Efficient training in the qubit case is more subtle and is discussed in Appendix B.1.

### 3 Quantum $k$ -Hypergraph Recurrent Neural Networks

We now introduce the hierarchy of quantum models that exhibit arbitrary polynomial expressivity separations over classical neural networks of the form discussed in Section 2.2. We call the  $k$ th level of this hierarchy of models  *$k$ -hypergraph recurrent neural networks* ( $k$ -HRNNs) for reasons that will soon become clear. We here give constructions for models implemented on qumodes (that is, in a CV setting) as it is a more natural quantum generalization of classical autoregressive networks. We give a similar construction for qubit-based models in Appendix B.

On qumodes, the  $k$ th level of this hierarchy of models includes networks composed of gates from the  $k$ th level of the *Clifford hierarchy*  $\mathcal{C}_k$ , which is defined inductively as operations that normalize the  $(k-1)$ st level of the hierarchy, with  $\mathcal{C}_1$  defined as the group of displacement operators. In general (for  $k > 2$ )  $\mathcal{C}_k$  is not a group as it is not closed under multiplication. As poly( $n$ )-dimensional dynamical Lie algebras

are a prerequisite for efficiently trainable quantum neural networks by the discussion of Section 2.3, we must restrict the structure of these models further in some way if they are to be practically implementable. We achieve this by considering quantum neural networks that consist of the sequential measurement of (parameterized)  *$k$ -uniform hypergraph state stabilizers* arranged in a specific way to yield trainable  $k$ -HRNNs. These states are reviewed in Appendix A.2, but knowledge of them is not required for the discussion here. Unless otherwise stated, we assume that  $k$  is constant with respect to  $n$ .

We consider qumode  $k$ -HRNNs in the autoregressive model framework discussed in Section 2.2 and as diagrammed in Figure 1(a). An ancillary input system on  $m$  qumodes indexed by  $\mathcal{M}$  is considered jointly with an  $n$ -qumode latent space indexed by  $\mathcal{N}$  along with an  $o$ -qumode output space indexed by  $\mathcal{O}$ . At each time step, a unitary  $U = \exp(-i\hat{H}) \exp(-i\hat{G})$  is applied on the joint space, where:

$$\hat{G} = \sum_{\substack{b \in \mathcal{N} \\ \bar{i} \in C_{\mathcal{M},k}}} \phi_{b,\bar{i}} \hat{q}_{\bar{i}} \otimes \hat{p}_b, \quad (8)$$

$$\hat{H} = \sum_{c \in \mathcal{O}} \hat{p}_c \otimes \left( \sum_{b \in \mathcal{N}} \gamma_{c,b} \hat{p}_b + \sum_{\bar{j} \in C_{\mathcal{N},k-1}} \theta_{c,\bar{j}} \hat{q}_{\bar{j}} \right). \quad (9)$$

Here,  $C_{\mathcal{A},k-1}$  is the set of multisets indexing all monomials through degree  $k-1$  with indices in  $\mathcal{A}$  and  $\hat{q}_{\bar{j}}$  the associated monomial of  $\hat{q}$  operators. The choice of inputs to the  $\mathcal{M}$  and  $\mathcal{O}$  registers are arbitrary (but fixed), as well as the choice for the initial state of the  $\mathcal{N}$  register. An example of a  $k$ -HRNN unit cell is sketched in Figure 2(a). As we show in Appendix D, a CV  $k$ -HRNN is a quantization of an RNN obeying the update rules:

$$\boldsymbol{\lambda}_{i+1} = \boldsymbol{\lambda}_i + \boldsymbol{f}(\boldsymbol{x}_i), \quad (10)$$

$$\boldsymbol{y}_i = \boldsymbol{g}(\boldsymbol{\lambda}_{i+1}), \quad (11)$$

where analytic functions  $\boldsymbol{f}, \boldsymbol{g}$  are approximated by degree- $(k-1)$  polynomials via their Taylor series.

As motivated in the beginning of this Section, qumode  $k$ -HRNNs have a dynamical Lie algebra with dimension scaling polynomially in the system size (for any constant  $m, k, o$ ). This is due to the degree of monomials in quadrature operators produced via the Lie bracket on terms in  $\hat{G}, \hat{H}$  being bounded by  $m + o + k - 1$ . This is easy to see as

$$\left[ \hat{p}_i, \hat{q}_{\bar{j}} \right] \propto \delta_{i \in \bar{j}} \hat{q}_{\bar{j} \setminus \{i\}}. \quad (12)$$

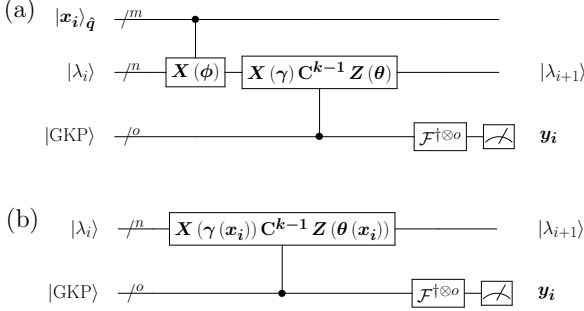


Figure 2: (a) A sketch of an example of a  $k$ -hypergraph recurrent neural network ( $k$ -HRNN) unit cell on qumodes as described in Section 3. The model is a quantization of a classical recurrent neural network, with structure of the form of Figure 1(a). Control units are in the position basis and  $|\text{GKP}\rangle$  represents a GKP state squeezed in the momentum basis.  $\mathbf{X}$  and  $\mathbf{Z}$  represent tensor products of displacement operators in  $\hat{p}$  and  $\hat{q}$ , respectively.  $\mathbf{x}_i$  is the input for this unit cell of the  $k$ -HRNN—given as a position-squeezed state  $|\mathbf{x}_i\rangle_{\hat{q}}$ —and  $\mathbf{y}_i$  its output. (b) An alternative construction of a  $k$ -HRNN cell where the parameters are promoted to parameterized functions of the input.

This immediately implies the efficient trainability of the model class using the, e.g., MMD loss function, as discussed in Section 2.3. We emphasize that though our model is efficiently trainable there may not be a time-complexity quantum-classical separation during training, i.e., the main result discussed in Section 4 should be interpreted as a quantum-classical resource separation only during inference. We further discuss this subtlety in Appendix E.3.

One nice property of this construction of an HRNN unit cell is that it is a member of (a natural qumode extension of)  $\text{QNC}_{\text{wf}}^0$ , that is, it can be implemented in constant depth on a quantum computer assuming access to quantum fan-out (or logarithmic depth if not) (Moore & Nilsson, 2001; 1998; Høyer & Špalek, 2005). This is easily observed from the Zassenhaus formula (Casas et al., 2012) using the commutation relation of equation (12):

$$\exp(-i\hat{H}) = \exp(-i\hat{H}_p) \exp(-i\hat{H}_q), \quad (13)$$

where  $\hat{H}_p$  and  $\hat{H}_q$  are each a sum of poly( $n$ )  $k$ -local commuting terms. This is distinguished from previously known quantum-classical communication complexity separations where the quantum computational

complexity grows exponentially in the communication complexity (Raz, 1999; Buhrman et al., 2001; Le Gall, 2006; Gavinsky et al., 2007; Gupta et al., 2023; Kallaugh et al., 2023; Manna et al., 2024). In Appendix E we strengthen this further and discuss an online version of the task which achieves a constant circuit complexity (i.e., circuit size, not just depth).

The introduction of a quantum input register indexed by  $\mathcal{M}$  allows the  $k$ -HRNN to be interpreted as a quantization of a classical RNN. However, in practice, QNNs are often implemented (or theoretically considered) such that their inputs are given implicitly in the network structure itself rather than as a quantum state in a new register (Killoran et al., 2019). More formally, the  $\phi_{b,\bar{i}}$  can be fixed to 0 and, rather than directly training the set of  $\gamma_{c,b}$  and  $\theta_{c,\bar{j}}$ , one can consider  $\gamma, \theta$  to be trainable functions of the input. This allows the QNN to be implemented with fewer quantum resources than otherwise would be required. A diagram illustrating this idea is given in Figure 2(b). In the remainder of our discussion we will implicitly consider this setting.

## 4 Arbitrary Polynomial Expressivity Separations Over Classical Neural Networks

### 4.1 $(\ell, n, k)$ -Hypergraph Stabilizer Measurement Translation

Having introduced  $k$ -HRNNs, we now describe the classical sequence modeling task with which we will prove our separation. The exact description of the task is slightly technical and is deferred to Appendix C.1; here we give an informal description. We once again focus on the CV version of the task here, with a qubit-based analog discussed informally in Appendix B.2 and formally in Appendix C.1.

The task we consider we call  $(\ell, n, k)$ -hypergraph stabilizer measurement translation ( $(\ell, n, k)$ -HSMT). Unless otherwise stated, we assume that  $k$  is constant with respect to  $n$ . For  $(\ell, n, k)$ -HSMT, we consider  $\ell$ -long input sequences

$$\mathbf{x} = (\mathbf{x}_1, \dots, \mathbf{x}_\ell)^\top \quad (14)$$

composed of classical descriptions of qumode  $k$ -uniform hypergraph state stabilizer generators:

$$s_b = \sum_{b \in \mathcal{N}} \gamma_b \hat{p}_b + \sum_{\bar{j} \in C_{\mathcal{N}, k-1}} \theta_{\bar{j}} \hat{q}_{\bar{j}} \quad (15)$$

on some  $n$ -qumode space indexed by  $\mathcal{N}$ . A translation

$$\mathbf{y} = (\mathbf{y}_1, \dots, \mathbf{y}_\ell)^\top \quad (16)$$

of  $\mathbf{x}$  is considered *correct* under the  $(\ell, n, k)$ -HSMT if it describes a sequence of measurement results that, according to the postulates of quantum mechanics, could have resulted from the sequential measurements of the observables described by  $\mathbf{x}_i$  when beginning in the squeezed state  $|\mathbf{0}\rangle_{\hat{a}}$ . More formally, we consider the sampling from the conditional distribution  $p(\mathbf{y} | \mathbf{x})$  of measurement outcomes given the measurement sequence described by  $\mathbf{x}$  on a quantum mechanical system beginning in a fixed state, where we only require sampling from  $p(\mathbf{y} | \mathbf{x})$  to *any* finite cross entropy. By construction, the  $k$ -HRNN defined in Section 3 can perform this task perfectly with only  $n$  qumodes in its latent space.

## 4.2 Expressivity Separations

We now give memory lower bounds on classical neural networks performing  $(\ell, n, k)$ -HSMT to a finite backward cross entropy. We here only give a sketch of our arguments and leave detailed and full proofs for Appendix C. Our main results follow from two facts that we prove:

**Proposition 4.1.** *For some  $\ell \geq 4n$ , there exist sequences in the  $(\ell, n, k)$ -HSMT task with completely distinct translations corresponding to antidistinguishing measurement sequences composed of (classical descriptions of) the measurement of contextual  $k$ -uniform hypergraph state stabilizers.*

“Antidistinguishing measurement sequences” are those which, given  $r$  candidates for a given quantum state, rule out one candidate with certainty; they arise as witnesses of quantum contextuality in quantum pseudo-telepathy games (Leifer, 2014). By “completely distinct translations” we mean the supports of the associated conditional distributions according to the  $(\ell, n, k)$ -HSMT task are disjoint.

**Proposition 4.2.** *Any classical neural network satisfying Assumptions 2.1 and 2.2 with latent space dimension less than  $\binom{n}{k} - 1$  induces a fiber bundle structure on some subspace of inputs, with fibers containing sequences with distinct translations in the  $(\ell, n, k)$ -HSMT task.*

That is, the classical neural network projects certain sequences with distinct translations under the  $(\ell, n, k)$ -HSMT task to the same point in its latent space.

Table 1: An example of quantum contextuality using a Mermin–Peres magic square (Mermin, 1990). All operators in each row and column commute. Additionally, the product of each row and column is the identity operator, except for the final column, which gives minus the identity. Thus, definite classical values cannot be assigned to each operator without yielding a contradiction. A more general form of this construction is used to construct antidistinguishing measurement sequences for hypergraph states, which is used to prove Proposition 4.1.

$X_1$	$X_2$	$X_1 X_2$
$X_1 Z_2$	$Z_1 X_2$	$-X_1 Z_1 X_2 Z_2$
$Z_2$	$Z_1$	$Z_1 Z_2$

Before proceeding with a proof sketch, we give some intuition behind these two Propositions—as well as their implications—by considering  $k = 2$  as a concrete example.

### 4.2.1 Intuition Behind Proposition 4.1

Proposition 4.1 with  $k = 2$  posits the existence of antidistinguishing measurement sequences composed of the sequential measurement of graph state stabilizers. As a simple example of this phenomenon for  $n = 2$  qubits, consider the graph states:

$$|\psi_1\rangle = |++\rangle, \quad |\psi_2\rangle = CZ_{1,2}|++\rangle, \quad (17)$$

along with a reference state  $|\psi_0\rangle = |00\rangle$ . Stabilizers of these three states are written in the rows of Table 1. Note that the rows and columns all multiply to the identity outside of the third column, which multiplies to minus the identity. This is a famous example of a *Mermin–Peres magic square* (Mermin, 1990): no classical assignment of these observables are consistent with the parity constraints enforced by their products even though each row and column of operators are mutually commuting. This is a manifestation of the phenomenon of *quantum contextuality*, namely, classical assignments of values to observables cannot yield measurement statistics consistent with quantum mechanics. This immediately yields a so-called *antidistinguishing measurement sequence* (Leifer, 2014). That is, a measurement sequence that succeeds with certainty that determines which of  $|\psi_0\rangle, |\psi_1\rangle, |\psi_2\rangle$  a state is *not*. One such measurement sequence for this example is given by measuring  $Z_1 Z_2$  followed by  $X_1 X_2$ . For  $|\psi_0\rangle$  to not be antidistinguished, the first

measurement result must be  $+1$  as it stabilizes  $|\psi_0\rangle$ . As the three operators in the final column of Table 1 commute, the post-measurement states of  $|\psi_1\rangle, |\psi_2\rangle$  after measuring  $Z_1Z_2$  to be  $+1$  are respectively stabilized by  $X_1X_2, -X_1X_2$ . They are thus orthogonal and can be distinguished with certainty.

Why is the presence of antidistinguishing measurement sequences important? Let  $p(y_3, y_4 | |\psi_i\rangle)$  for  $i = 0, 1, 2$  be conditional distributions describing the measurement results  $y_3, y_4$  of the previously defined antidistinguishing measurement sequence. For  $i = 0$ , this distribution only has support on  $y_3 = +1$  as  $Z_1Z_2$  stabilizes  $|\psi_0\rangle$ . For  $i = 1$ , conditioned on  $y_3 = +1$ , the distribution only has support on  $y_4 = +1$  as previously described, and similarly for  $i = 2$  with  $y_4 = -1$ . It is easy to see that antidistinguishing measurement sequences correspond to *completely distinct translations*, that is,  $p(y_3, y_4 | |\psi_i\rangle)$  and  $p(y_3, y_4 | |\psi_j\rangle)$  (where  $j \neq i$ ) have an infinite cross entropy. The  $(\ell, n, k)$ -HSMT task is constructed to take advantage of this fact.

For general  $k$ —as well as for qumodes—the proof of the Proposition proceeds similarly to the logic laid out here, though now it requires the sequential measurement of hypergraph state stabilizers rather than graph state stabilizers. Formal proofs for qubits and qumodes are given in Appendix C.2 as the proofs of Lemmas C.1 and C.2, respectively.

#### 4.2.2 Intuition Behind Proposition 4.2

This now motivates a proof strategy: if one can show that a classical model with limited memory must share internal representations among sequences corresponding to the preparation of  $|\psi_0\rangle, |\psi_1\rangle, |\psi_2\rangle$ , for (at least) one of these sequences the model will sample from the incorrect distribution and achieve an infinite backward cross entropy on the  $(\ell, n, k)$ -HSMT task.

This is what we accomplish via a proof of Proposition 4.2 which relies on Assumptions 2.1 and 2.2. At a basic level, this Proposition is a statement that if the classical neural network is “sufficiently nice,” the  $\binom{n}{k} - 1$ -dimensional space of hypergraphs (up to an overall scaling of the hyperedge weights) cannot be injectively represented in the latent space of the network if it is of dimension less than  $\binom{n}{k} - 1$ . However, we require even more structure than this: we require that what is noninjectively mapped to some point in latent space are measurement sequences that have completely distinct translations in the sense of Proposition 4.1.

To achieve this we show that not only is a classical

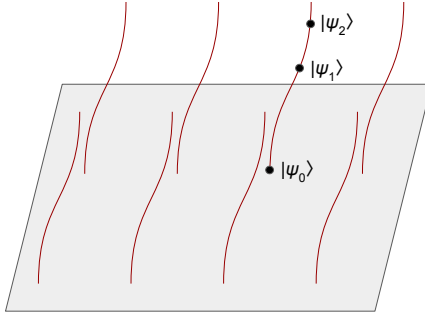


Figure 3: A representation of the fiber bundle structure induced on the input space by a given classical neural network of insufficient memory. The gray parallelogram represents the base space, and red lines represent fibers.  $|\psi_0\rangle, |\psi_1\rangle$ , and  $|\psi_2\rangle$  label input sequences describing the preparation of the associated states as described in Section 4.1. The classical neural network maps all points sharing a fiber to the same point in its latent space, and thus all input sequences sharing a fiber are indistinguishable to the neural network.

neural network map noninjective, but that it induces a *fiber bundle* structure on the space of inputs where the fibers are “sufficiently large” to contain input sequences with completely distinct translations. That is, we show that there exists a manifold structure on the input space where certain coordinates are locally projected out by the classical neural network, and that the size of this local region is lower-bounded. We give a sketch of this structure in Figure 3. Requiring this lower bound on the region size is what necessitates our Assumption 2.2, which requires the existence of a subspace of inputs where the Jacobian determinant of the neural network is not arbitrarily close to zero. Intuitively this requirement can be seen as a consequence of the inverse function theorem, as the neighborhood where it holds around a given point grows with the Jacobian determinant at that point. More formally we use a certain formulation of a “global implicit function theorem” described in the work of Rabier (1997).

Formal proofs of this Proposition differ depending on whether the task is qubit or qumode  $(\ell, n, k)$ -HSMT, and whether the classical model is an autoregressive model or an encoder-decoder model. They are given as Theorems C.3, C.4, C.5, and C.6, all stated and proved in Appendix C.



### 4.2.3 Main Result

Our main result follows from Propositions 4.1 and 4.2. As previously stated, our formal proofs and statements depend on whether the task is qubit or qumode  $(\ell, n, k)$ -HSMT, and whether the classical model is an autoregressive model or an encoder-decoder model. The formal proofs and statements are given across Theorems C.3, C.4, C.5, and C.6, all stated and proved in Appendix C. For simplicity, we here gloss over the details which distinguish these four Theorems and give a high-level proof sketch of our separations.

**Theorem 4.3** (Memory lower bound for  $(\ell, n, k)$ -HSMT, informal). *Consider the qubit or qumode  $(\ell, n, k)$ -HSMT task as described in Section 4.1 with  $\ell \geq 4n$ . A classical neural network satisfying Assumptions 2.1 and 2.2 must have latent space dimension at least  $\binom{n}{k} - 1$  to perform the  $(\ell, n, k)$ -HSMT task to any finite backward cross entropy. A  $k$ -HRNN of model size  $n$  can perform this task to zero error.*

*Proof sketch.* By Proposition 4.1, there exist inputs to the classical neural network corresponding to the preparation of hypergraph states with antidistinguishing measurement sequences. By Proposition 4.2, if the latent space of the neural network is of dimension less than  $\binom{n}{k} - 1$ , it induces a fiber bundle structure on the space of inputs with fibers “large enough” such that sequences satisfying Proposition 4.1 share a fiber. Namely, under the  $(\ell, n, k)$ -HSMT task, there exist sequences with completely distinct translations that are indistinguishable by the classical neural network. Thus, the network must get a translation incorrect for one of these three inputs, yielding an infinite backward cross entropy when attempting to perform the task. The fact that  $k$ -HRNNs of model size  $n$  can perform this task to zero error is discussed in Section 4.1.  $\square$

Throughout we have assumed that  $k$  is constant with respect to  $n$ ; in this setting, this separation is polynomial in  $n$ . We note here that if  $k$  is instead allowed to grow with  $n$  our results imply an exponential quantum-classical separation. The trade-off is that the resulting model is not efficiently trainable—by the discussion of Section 2.3—and the resulting model no longer has unit cells in QNC (Moore & Nilsson, 2001; 1998; Høyer & Špalek, 2005).

## 5 Conclusion

Our results construct a hierarchy quantum neural networks that are not only efficiently trainable, but also more expressive than classical neural networks by an arbitrary polynomial factor. Our introduced hierarchy of quantum models tracts nicely with experimental capabilities: given the ability to implement  $k$ -local gates, one can achieve an  $\Theta(n^k)$  memory separation over classical neural networks in performing the translation task we here introduce. This makes our hierarchy a natural fit for implementation on Rydberg atom-based quantum architectures which naturally implement circuits in  $\text{QNC}_{\text{wf}}^0$  in constant depth (Isenhower et al., 2011). Our model also has the benefit of being composed of operations for which error correction has successfully been experimentally demonstrated (Bluvstein et al., 2023). Cavity quantum electrodynamics (QED) systems are also a natural platform to implement our model, as coherent information from the CV degrees of freedom can be stored in the cavity while atomic degrees of freedom are read out to perform the necessary measurements (Kerman, 2013; Blais et al., 2021).

More work is required for demonstrating the practicality of our introduced advantage. First, our qubit-based models are only trainable under fairly stringent constraints on the trained parameters. Effectively, it requires restricting the quantum model such that it faithfully represents sequence data as weighted hypergraph states. Though loosening this assumption would be ideal, an alternative approach could be to consider scenarios where a hypergraph representation of the data is natural. A similar approach was taken in the work of Gokhale et al. (2022), where graph states were used as efficient representations of sequence data in the context of fingerprinting.

Secondly, we are only able to prove an arbitrary polynomial *memory* separation, not a time separation. Memory separations are natural in an online sequence learning setting, as discussed Appendix E, but classical circuit depth lower-bounds (other than the trivial  $\text{NC}^1$  we give in Appendix E.1) would be useful for broadening the scope of where one might expect a practical quantum advantage in sequence learning.

Finally, our protocol is here considered in a noise-free context, far from the experimental capabilities of most current quantum devices. However, our results follow from antidistinguishing measurement sequences similar to those seen in the setting of pseudo-telepathy games (Leifer, 2014), and previous work (Bravyi et al., 2020; Caha et al., 2023) has demonstrated instances

where quantum separations based on pseudo-telepathy games can be made noise resilient. We hope to explore these connections in future work.

HRNNs demonstrate that quantizing a very simple class of recurrent neural networks—those that update their latent state additively—is enough to achieve a large expressivity separation over classical neural networks on a sequence modeling task. Given the tremendous progress in the performance of large language models in recent years with the introduction of, for instance, GPT-3 (Brown et al., 2020) and GPT-4 (OpenAI, 2023), this begs the natural question: what can be achieved by quantizing more sophisticated classical models? We hope in the future to address this.

## Impact Statement

This paper presents work whose goal is to advance the field of Machine Learning. There are many potential societal consequences of our work, none which we feel must be specifically highlighted here.

## Acknowledgements

We thank Cameron Calcluth and Mikhail D. Lukin for helpful discussion. E.R.A. was funded in part by the Walter Burke Institute for Theoretical Physics at Caltech and in part by the DARPA ONISQ program (grant number W911NF2010021). X.G. acknowledges startup funding from JILA and CU Boulder.

## References

- Aaronson, S. and Gottesman, D. Improved simulation of stabilizer circuits. *Phys. Rev. A*, 70:052328, 2004. doi: 10.1103/PhysRevA.70.052328.
- Amin, M. H., Andriyash, E., Rolfe, J., Kulchyt-skiy, B., and Melko, R. Quantum Boltzmann machine. *Phys. Rev. X*, 8:021050, 2018. doi: 10.1103/PhysRevX.8.021050.
- Anschuetz, E. R. Critical points in quantum generative models. In Hofmann, K., Rush, A., Liu, Y., Finn, C., Choi, Y., and Deisenroth, M. (eds.), *International Conference on Learning Representations*. OpenReview, 2022. URL <https://openreview.net/forum?id=2f1z55GVQN>.
- Anschuetz, E. R. and Kiani, B. T. Quantum variational algorithms are swamped with traps. *Nat. Commun.*, 13:7760, 2022. doi: 10.1038/s41467-022-35364-5.
- Anschuetz, E. R., Bauer, A., Kiani, B. T., and Lloyd, S. Efficient classical algorithms for simulating symmetric quantum systems, 2022.
- Anschuetz, E. R., Hu, H.-Y., Huang, J.-L., and Gao, X. Interpretable quantum advantage in neural sequence learning. *PRX Quantum*, 4:020338, 2023. doi: 10.1103/PRXQuantum.4.020338.
- Arrasmith, A., Cerezo, M., Czarnik, P., Cincio, L., and Coles, P. J. Effect of barren plateaus on gradient-free optimization. *Quantum*, 5:558, 2021. ISSN 2521-327X. doi: 10.22331/q-2021-10-05-558.
- Babbush, R., McClean, J. R., Newman, M., Gidney, C., Boixo, S., and Neven, H. Focus beyond quadratic speedups for error-corrected quantum advantage. *PRX Quantum*, 2:010103, 2021. doi: 10.1103/PRXQuantum.2.010103.
- Biamonte, J., Wittek, P., Pancotti, N., Rebentrost, P., Wiebe, N., and Lloyd, S. Quantum machine learning. *Nature*, 549(7671):195–202, 2017. doi: 10.1038/nature23474.
- Blais, A., Grimsmo, A. L., Girvin, S. M., and Wallraff, A. Circuit quantum electrodynamics. *Rev. Mod. Phys.*, 93:025005, 2021. doi: 10.1103/RevModPhys.93.025005.
- Bluvstein, D., Evered, S. J., Geim, A. A., Li, S. H., Zhou, H., Manovitz, T., Ebadi, S., Cain, M., Kalinowski, M., Hangleiter, D., et al. Logical quantum processor based on reconfigurable atom arrays. *Nature*, pp. 1–3, 2023. doi: 10.1038/s41586-023-06927-3.
- Booth, R. I., Chabaud, U., and Emeriau, P.-E. Contextuality and Wigner negativity are equivalent for continuous-variable quantum measurements. *Phys. Rev. Lett.*, 129:230401, 2022. doi: 10.1103/PhysRevLett.129.230401.
- Bravyi, S., Gosset, D., Koenig, R., and Tomamichel, M. Quantum advantage with noisy shallow circuits. *Nat. Phys.*, 16(10):1040–1045, 2020. doi: 10.1038/s41567-020-0948-z.
- Brown, T. et al. Language models are few-shot learners. In Larochelle, H., Ranzato,

- M., Hadsell, R., Balcan, M., and Lin, H. (eds.), *Proceedings of the 34th International Conference on Neural Information Processing Systems*, NIPS'20, pp. 1877–1901, Red Hook, NY, USA, 2020. Curran Associates, Inc. URL <https://papers.nips.cc/paper/2020/hash/1457c0d6bfc4967418bfb8ac142f64a-Abstract.html>.
- Buhrman, H., Cleve, R., Watrous, J., and de Wolf, R. Quantum fingerprinting. *Phys. Rev. Lett.*, 87: 167902, 2001. doi: 10.1103/PhysRevLett.87.167902.
- Caha, L., Coiteux-Roy, X., and Koenig, R. A colossal advantage: 3D-local noisy shallow quantum circuits defeat unbounded fan-in classical circuits, 2023.
- Calcluth, C., Ferraro, A., and Ferrini, G. Efficient simulation of Gottesman-Kitaev-Preskill states with Gaussian circuits, 2022.
- Casas, F., Murua, A., and Nadinic, M. Efficient computation of the zassenhaus formula. *Comput. Phys. Commun.*, 183(11):2386–2391, 2012. ISSN 0010-4655. doi: 10.1016/j.cpc.2012.06.006.
- Cerezo, M. and Coles, P. J. Higher order derivatives of quantum neural networks with barren plateaus. *Quantum Sci. Technol.*, 6(3):035006, 2021. doi: 10.1088/2058-9565/abf51a.
- Cerezo, M., Sone, A., Volkoff, T., Cincio, L., and Coles, P. J. Cost function dependent barren plateaus in shallow parametrized quantum circuits. *Nat. Commun.*, 12(1):1791–1802, 2021. doi: 10.1038/s41467-021-21728-w.
- Cerezo, M., Larocca, M., García-Martín, D., Diaz, N. L., Braccia, P., Fontana, E., Rudolph, M. S., Bermejo, P., Ijaz, A., Thanasilp, S., Anschuetz, E. R., and Holmes, Z. Does provable absence of barren plateaus imply classical simulability? or, why we need to rethink variational quantum computing, 2023.
- Chaudhari, P. A. *A Picture of the Energy Landscape of Deep Neural Networks*. PhD thesis, University of California, Los Angeles, 2018. URL <https://escholarship.org/uc/item/26h5787r>.
- Cho, K., van Merriënboer, B., Gulcehre, C., Bahdanau, D., Bougares, F., Schwenk, H., and Bengio, Y. Learning phrase representations using RNN encoder–decoder for statistical machine translation. In Moschitti, A., Pang, B., and Daelemans, W. (eds.), *Proceedings of the 2014 Conference on Empirical Methods in Natural Language Processing (EMNLP)*, pp. 1724–1734, Doha, 2014. Association for Computational Linguistics. doi: 10.3115/v1/D14-1179.
- Choromanska, A., Henaff, M., Mathieu, M., Arous, G. B., and LeCun, Y. The loss surfaces of multi-layer networks. In Lebanon, G. and Vishwanathan, S. V. N. (eds.), *Proceedings of the Eighteenth International Conference on Artificial Intelligence and Statistics*, volume 38 of *Proceedings of Machine Learning Research*, pp. 192–204, San Diego, CA, USA, 2015. PMLR. URL <http://proceedings.mlr.press/v38/choromanska15.html>.
- Coyle, B., Mills, D., Danos, V., and Kashefi, E. The Born supremacy: quantum advantage and training of an Ising Born machine. *npj Quantum Inf.*, 6(1): 1–11, 2020. doi: 10.1038/s41534-020-00288-9.
- Dixit, R., Gurbuzbalaban, M., and Bajwa, W. U. Accelerated gradient methods for nonconvex optimization: Escape trajectories from strict saddle points and convergence to local minima, 2023.
- Domingos, P. and Hulten, G. Mining high-speed data streams. In Ramakrishnan, R., Stolfo, S., Bayardo, R., and Parsa, I. (eds.), *Proceedings of the Sixth ACM SIGKDD International Conference on Knowledge Discovery and Data Mining*, KDD '00, pp. 71–80, New York, NY, USA, 2000. Association for Computing Machinery. ISBN 1581132336. doi: 10.1145/347090.347107.
- Du, Y., Hsieh, M.-H., Liu, T., and Tao, D. Expressive power of parametrized quantum circuits. *Phys. Rev. Research*, 2:033125, 2020. doi: 10.1103/PhysRevResearch.2.033125.
- Duan, R., Wu, H., and Zhou, R. Faster matrix multiplication via asymmetric hashing, 2022.
- Fontana, E., Herman, D., Chakrabarti, S., Kumar, N., Yalovetzky, R., Heredge, J., Sureshbabu, S. H., and Pistoia, M. The adjoint is all you need: Characterizing barren plateaus in quantum ansätze, 2023.
- Gaber, M. M., Zaslavsky, A., and Krishnaswamy, S. Mining data streams: A review. *SIGMOD Rec.*, 34(2):18–26, 2005. ISSN 0163-5808. doi: 10.1145/1083784.1083789.

- Gama, J. A survey on learning from data streams: current and future trends. *Prog. Artif. Intell.*, 1(1): 45–55, 2012. doi: 10.1007/s13748-011-0002-6.
- Gao, X., Zhang, Z.-Y., and Duan, L.-M. A quantum machine learning algorithm based on generative models. *Sci. Adv.*, 4(12):eaat9004, 2018. doi: 10.1126/sciadv.aat9004.
- Gavinsky, D., Kempe, J., Kerenidis, I., Raz, R., and de Wolf, R. Exponential separations for one-way quantum communication complexity, with applications to cryptography. In Johnson, D. and Feige, U. (eds.), *Proceedings of the Thirty-Ninth Annual ACM Symposium on Theory of Computing*, STOC '07, pp. 516–525, New York, NY, USA, 2007. Association for Computing Machinery. ISBN 9781595936318. doi: 10.1145/1250790.1250866.
- Gokhale, P., Anschuetz, E. R., Campbell, C., Chong, F. T., Dahl, E. D., Frederick, P., Jones, E. B., Hall, B., Issa, S., Goiporia, P., Lee, S., Noell, P., Omole, V., Owusu-Antwi, D., Perlin, M. A., Rines, R., Saffman, M., Smith, K. N., and Tomesh, T. SupercheQ: Quantum advantage for distributed databases, 2022.
- Goodfellow, I. J., Pouget-Abadie, J., Mirza, M., Xu, B., Warde-Farley, D., Ozair, S., Courville, A., and Bengio, Y. Generative adversarial nets. In Ghahramani, Z., Welling, M., Cortes, C., Lawrence, N., and Weinberger, K. (eds.), *Proceedings of the 27th International Conference on Neural Information Processing Systems - Volume 2*, NIPS'14, pp. 2672–2680, Red Hook, NY, USA, 2014. Curran Associates, Inc. URL [https://papers.nips.cc/paper\\_files/paper/2014/hash/5ca3e9b122f61f8f06494c97b1afccf3-Abstract.html](https://papers.nips.cc/paper_files/paper/2014/hash/5ca3e9b122f61f8f06494c97b1afccf3-Abstract.html).
- Gottesman, D. and Chuang, I. L. Demonstrating the viability of universal quantum computation using teleportation and single-qubit operations. *Nature*, 402(6760):390–393, 1999. doi: 10.1038/46503.
- Gottesman, D., Kitaev, A., and Preskill, J. Encoding a qubit in an oscillator. *Phys. Rev. A*, 64:012310, 2001. doi: 10.1103/PhysRevA.64.012310.
- Gupta, S., Saha, D., Xu, Z.-P., Cabello, A., and Majumdar, A. S. Quantum contextuality provides communication complexity advantage. *Phys. Rev. Lett.*, 130:080802, 2023. doi: 10.1103/PhysRevLett.130.080802.
- Havlíček, V., Córcoles, A. D., Temme, K., Harrow, A. W., Kandala, A., Chow, J. M., and Gambetta, J. M. Supervised learning with quantum-enhanced feature spaces. *Nature*, 567(7747):209–212, 2019. doi: 10.1038/s41586-019-0980-2.
- Hochreiter, S. and Schmidhuber, J. Long short-term memory. *Neural Comput.*, 9(8):1735–1780, 1997. ISSN 0899-7667. doi: 10.1162/neco.1997.9.8.1735.
- Holmes, Z., Sharma, K., Cerezo, M., and Coles, P. J. Connecting ansatz expressibility to gradient magnitudes and barren plateaus. *PRX Quantum*, 3:010313, 2022. doi: 10.1103/PRXQuantum.3.010313.
- Hopfield, J. J. Neural networks and physical systems with emergent collective computational abilities. *Proc. Natl. Acad. Sci. U.S.A.*, 79(8):2554–2558, 1982. ISSN 0027-8424. doi: 10.1073/pnas.79.8.2554.
- Høyer, P. and Špalek, R. Quantum fan-out is powerful. *Theory Comput.*, 1(5):81–103, 2005. doi: 10.4086/toc.2005.v001a005.
- Isenhower, L., Saffman, M., and Mølmer, K. Multi-bit  $C_k$  NOT quantum gates via Rydberg blockade. *Quantum. Inf. Process.*, 10:755–770, 2011. doi: 10.1007/s11128-011-0292-4.
- Kallaugher, J., Parekh, O., and Voronova, N. Exponential quantum space advantage for approximating maximum directed cut in the streaming model, 2023.
- Kerman, A. J. Quantum information processing using quasiclassical electromagnetic interactions between qubits and electrical resonators. *New J. Phys.*, 15(12):123011, 2013. doi: 10.1088/1367-2630/15/12/123011.
- Killoran, N., Bromley, T. R., Arrazola, J. M., Schuld, M., Quesada, N., and Lloyd, S. Continuous-variable quantum neural networks. *Phys. Rev. Research*, 1:033063, 2019. doi: 10.1103/PhysRevResearch.1.033063.
- Kurochkin, S. V. Neural network with smooth activation functions and without bottlenecks is almost surely a Morse function. *Comput. Math. and Math. Phys.*, 61(7):1162–1168, 2021. doi: 10.1134/S0965542521070101.
- Larocca, M., Czarnik, P., Sharma, K., Muraleedharan, G., Coles, P. J., and Cerezo, M. Diagnosing barren

- plateaus with tools from quantum optimal control. *Quantum*, 6:824, 2022a. ISSN 2521-327X. doi: 10.22331/q-2022-09-29-824.
- Larocca, M., Sauvage, F., Sbahi, F. M., Verdon, G., Coles, P. J., and Cerezo, M. Group-invariant quantum machine learning. *PRX Quantum*, 3:030341, 2022b. doi: 10.1103/PRXQuantum.3.030341.
- Larocca, M., Ju, N., García-Martín, D., Coles, P. J., and Cerezo, M. Theory of overparametrization in quantum neural networks. *Nat. Comput. Sci.*, 3(6): 542–551, 2023. doi: 10.1038/s43588-023-00467-6.
- Le Gall, F. Exponential separation of quantum and classical online space complexity. In Gibbons, P. B. and Vishkin, U. (eds.), *Proceedings of the Eighteenth Annual ACM Symposium on Parallelism in Algorithms and Architectures*, SPAA '06, pp. 67–73, New York, NY, USA, 2006. Association for Computing Machinery. ISBN 1595934529. doi: 10.1145/1148109.1148119.
- Leifer, M. Is the quantum state real? an extended review of  $\psi$ -ontology theorems. *Quanta*, 3(1):67–155, 2014. ISSN 1314-7374. doi: 10.12743/quanta.v3i1.22.
- Liu, N., Thompson, J., Weedbrook, C., Lloyd, S., Vedral, V., Gu, M., and Modi, K. Power of one qumode for quantum computation. *Phys. Rev. A*, 93:052304, 2016. doi: 10.1103/PhysRevA.93.052304.
- Liu, Y., Arunachalam, S., and Temme, K. A rigorous and robust quantum speed-up in supervised machine learning. *Nat. Phys.*, 17(9):1013–1017, 2021. doi: 10.1038/s41567-021-01287-z.
- Lloyd, S. and Weedbrook, C. Quantum generative adversarial learning. *Phys. Rev. Lett.*, 121:040502, 2018. doi: 10.1103/PhysRevLett.121.040502.
- Manna, S., Chaturvedi, A., and Saha, D. Unbounded quantum advantage in communication complexity measured by distinguishability, 2024.
- Mari, A. and Eisert, J. Positive Wigner functions render classical simulation of quantum computation efficient. *Phys. Rev. Lett.*, 109:230503, 2012. doi: 10.1103/PhysRevLett.109.230503.
- McClean, J. R., Boixo, S., Smelyanskiy, V. N., Babbush, R., and Neven, H. Barren plateaus in quantum neural network training landscapes. *Nat. Commun.*, 9(1):4812, 2018. doi: 10.1038/s41467-018-07090-4.
- Mei, S., Bai, Y., and Montanari, A. The landscape of empirical risk for nonconvex losses. *Ann. Stat.*, 46(6A):2747–2774, 2018. ISSN 00905364, 21688966. doi: 10.1214/17-AOS1637.
- Mermin, N. D. Simple unified form for the major no-hidden-variables theorems. *Phys. Rev. Lett.*, 65: 3373–3376, 1990. doi: 10.1103/PhysRevLett.65.3373.
- Mokhtari, A., Ozdaglar, A., and Jadbabaie, A. Efficient nonconvex empirical risk minimization via adaptive sample size methods. In Chaudhuri, K. and Sugiyama, M. (eds.), *Proceedings of the Twenty-Second International Conference on Artificial Intelligence and Statistics*, volume 89 of *Proceedings of Machine Learning Research*, pp. 2485–2494, Naha, Japan, 2019. PMLR. URL <https://proceedings.mlr.press/v89/mokhtari19a.html>.
- Moore, C. and Nilsson, M. Some notes on parallel quantum computation, 1998.
- Moore, C. and Nilsson, M. Parallel quantum computation and quantum codes. *SIAM J. Comput.*, 31(3): 799–815, 2001. doi: 10.1137/S0097539799355053.
- Napp, J. Quantifying the barren plateau phenomenon for a model of unstructured variational ansätze, 2022.
- Nguyen, Q. T., Schatzki, L., Braccia, P., Ragone, M., Coles, P. J., Sauvage, F., Larocca, M., and Cerezo, M. Theory for equivariant quantum neural networks, 2022.
- Nielsen, M. A. and Chuang, I. L. *The quantum Fourier transform and its applications*, pp. 216–247. Cambridge University Press, Cambridge, 2010. doi: 10.1017/CBO9780511976667.009.
- OpenAI. GPT-4 technical report, 2023.
- Perdomo-Ortiz, A., Benedetti, M., Realpe-Gómez, J., and Biswas, R. Opportunities and challenges for quantum-assisted machine learning in near-term quantum computers. *Quantum Sci. Technol.*, 3(3): 030502, 2018. doi: 10.1088/2058-9565/aab859.
- Prabhavalkar, R., Rao, K., Sainath, T. N., Li, B., Johnson, L., and Jaitly, N. A comparison of sequence-to-sequence models for speech recognition.

- In Lacerda, F. (ed.), *Proc. Interspeech 2017*, pp. 939–943, Red Hook, NY, USA, 2017. Curran Associates, Inc. doi: 10.21437/Interspeech.2017-233.
- Rabier, P. J. Ehresmann fibrations and Palais-Smale conditions for morphisms of Finsler manifolds. *Ann. Math.*, 146(3):647–691, 1997. ISSN 0003486X. doi: 10.2307/2952457.
- Ragone, M., Braccia, P., Nguyen, Q. T., Schatzki, L., Coles, P. J., Sauvage, F., Larocca, M., and Cerezo, M. Representation theory for geometric quantum machine learning, 2022.
- Ragone, M., Bakalov, B. N., Sauvage, F., Kemper, A. F., Marrero, C. O., Larocca, M., and Cerezo, M. A unified theory of barren plateaus for deep parametrized quantum circuits, 2023.
- Raz, R. Exponential separation of quantum and classical communication complexity. In *Proceedings of the Thirty-First Annual ACM Symposium on Theory of Computing*, STOC '99, pp. 358–367, New York, NY, USA, 1999. Association for Computing Machinery. ISBN 1581130678. doi: 10.1145/301250.301343.
- Rudolph, M. S., Lerch, S., Thanasilp, S., Kiss, O., Vallecorsa, S., Grossi, M., and Holmes, Z. Trainability barriers and opportunities in quantum generative modeling, 2023.
- Schuld, M. and Killoran, N. Quantum machine learning in feature Hilbert spaces. *Phys. Rev. Lett.*, 122:040504, 2019. doi: 10.1103/PhysRevLett.122.040504.
- Schuld, M., Sinayskiy, I., and Petruccione, F. An introduction to quantum machine learning. *Contemp. Phys.*, 56(2):172–185, 2015. doi: 10.1080/00107514.2014.964942.
- Shi, B., Su, W. J., and Jordan, M. I. On learning rates and Schrödinger operators, 2020.
- Somma, R., Barnum, H., Ortiz, G., and Knill, E. Efficient solvability of hamiltonians and limits on the power of some quantum computational models. *Phys. Rev. Lett.*, 97:190501, 2006. doi: 10.1103/PhysRevLett.97.190501.
- Strassen, V. Gaussian elimination is not optimal. *Numer. Math.*, 13(4):354–356, 1969. doi: 10.1007/BF02165411.
- Sutskever, I., Vinyals, O., and Le, Q. V. Sequence to sequence learning with neural networks. In Ghahramani, Z., Welling, M., Cortes, C., and Lawrence, N. (eds.), *Proceedings of the 27th International Conference on Neural Information Processing Systems - Volume 2*, NIPS'14, pp. 3104–3112, Red Hook, NY, USA, 2014. Curran Associates, Inc. URL [https://papers.nips.cc/paper\\_files/paper/2014/hash/a14ac55a4f27472c5d894ec1c3c743d2-Abstract.html](https://papers.nips.cc/paper_files/paper/2014/hash/a14ac55a4f27472c5d894ec1c3c743d2-Abstract.html).
- Sweke, R., Seifert, J.-P., Hangleiter, D., and Eisert, J. On the Quantum versus Classical Learnability of Discrete Distributions. *Quantum*, 5:417, 2021. ISSN 2521-327X. doi: 10.22331/q-2021-03-23-417.
- Takeuchi, Y., Mantri, A., Morimae, T., Mizutani, A., and Fitzsimons, J. F. Resource-efficient verification of quantum computing using serfling’s bound. *npj Quantum Inf.*, 5(1):27, 2019. doi: 10.1038/s41534-019-0142-2.
- Vaswani, A., Shazeer, N., Parmar, N., Uszkoreit, J., Jones, L., Gomez, A. N., Kaiser, L., and Polosukhin, I. Attention is all you need. In Guyon, I., Luxburg, U. V., Bengio, S., Wallach, H., Fergus, R., Vishwanathan, S., and Garnett, R. (eds.), *Proceedings of the 31st International Conference on Neural Information Processing Systems*, NIPS'17, pp. 6000–6010, Red Hook, NY, USA, 2017. Curran Associates, Inc. ISBN 9781510860964. URL [https://papers.nips.cc/paper\\_files/paper/2017/hash/3f5ee243547dee91fbd053c1c4a845aa-Abstract.html](https://papers.nips.cc/paper_files/paper/2017/hash/3f5ee243547dee91fbd053c1c4a845aa-Abstract.html).
- Vinyals, O., Toshev, A., Bengio, S., and Erhan, D. Show and tell: A neural image caption generator. In Barnard, K., Bischof, H., Felzenszwalb, P., Forsyth, D., Lazebnik, S., and Matas, J. (eds.), *2015 IEEE Conference on Computer Vision and Pattern Recognition (CVPR)*, pp. 3156–3164, Red Hook, NY, USA, 2015. Curran Associates, Inc. doi: 10.1109/CVPR.2015.7298935.
- Wan, K., Choi, S., Kim, I. H., Shutt, N., and Hayden, P. Fault-tolerant qubit from a constant number of components. *PRX Quantum*, 2:040345, 2021. doi: 10.1103/PRXQuantum.2.040345.
- Webster, M. A., Brown, B. J., and Bartlett, S. D. The XP stabiliser formalism: a generalisation of the Pauli stabiliser formalism with arbitrary phases.

*Quantum*, 6:815, 2022. ISSN 2521-327X. doi: 10.22331/q-2022-09-22-815.

Yang, J., Hu, W., and Li, C. J. On the fast convergence of random perturbations of the gradient flow. *Asymptot. Anal.*, 122(3–4):371–393, 2021. doi: 10.3233/ASY-201622.

# A Weighted Hypergraph States

## A.1 Qubit Weighted Hypergraph States

We here give a bevy of facts about *qubit weighted hypergraph states*. Though first introduced in the work of Webster et al. (2022) in the context of how they map to the XP stabilizer formalism, we here directly consider a stabilizer formalism of such states.

We first review the definition of qubit weighted hypergraph states, focusing for simplicity on cases where the associated hypergraphs are *k-uniform hypergraphs*; namely, their only nontrivial hyperedges are associated with cardinality  $k$  subsets of vertices. Let  $G$  be a  $k$ -uniform weighted hypergraph with hyperedges labeled by sets  $\bar{v}$  and with associated hyperedge weights  $e_{\bar{v}}$ . We denote as  $|G\rangle$  the *qubit k-uniform weighted hypergraph state associated with G*:

$$|G\rangle \equiv \prod_{\bar{v} \in G} U_{\bar{v}}(e_{\bar{v}}) |+\rangle^{\otimes n}, \quad (18)$$

where:

$$U_{\bar{v}}(e_{\bar{v}}) \equiv \exp\left(i\pi e_{\bar{v}} \prod_{i \in \bar{v}} \frac{I - Z_i}{2}\right) \quad (19)$$

is a power of the multi-controlled phase gate  $C^k Z_{\bar{v}}$ , i.e.,

$$C^k Z_{\bar{v}} = U_{\bar{v}}(1). \quad (20)$$

It is easy to check the commutation relations when  $i \in \bar{v}$ :

$$X_i U_{\bar{v}}(e_{\bar{v}}) = U_{\bar{v} \setminus \{i\}}(e_{\bar{v}}) U_{\bar{v}}(-e_{\bar{v}}) X_i, \quad (21)$$

$$U_{\bar{v}}(e_{\bar{v}}) X_i = X_i U_{\bar{v} \setminus \{i\}}(e_{\bar{v}}) U_{\bar{v}}(-e_{\bar{v}}). \quad (22)$$

By construction,  $|G\rangle$  is the mutual  $+1$  eigenstate of the commuting operators:

$$\begin{aligned} s_i &= \prod_{\bar{v} \ni i} U_{\bar{v}}(e_{\bar{v}}) X_i \left( \prod_{\bar{v} \ni i} U_{\bar{v}}(e_{\bar{v}}) \right)^\dagger \\ &= X_i \prod_{\bar{v} \ni i} U_{\bar{v} \setminus \{i\}}(e_{\bar{v}}) U_{\bar{v}}(-2e_{\bar{v}}) \\ &= \left( \prod_{\bar{v} \ni i} U_{\bar{v} \setminus \{i\}}(-e_{\bar{v}}) U_{\bar{v}}(2e_{\bar{v}}) \right) X_i. \end{aligned} \quad (23)$$

From this it is immediately clear that the  $s_i$  are their own inverses:

$$s_i^2 = I. \quad (24)$$

Thus,

$$s_i = \exp\left(-i\frac{\pi}{2}\right) \exp\left(i\frac{\pi}{2}s_i\right) \quad (25)$$

and in particular  $|G\rangle$  is also stabilized by all powers  $s_i^\alpha$ . It is also apparent from equation (23) that the  $s_i$  are Hermitian.

We now consider the special case where  $G$  has only a single hyperedge  $\bar{v}$ . Consider the stabilizer of  $|G\rangle$ :

$$s_{\bar{v}} \equiv \prod_{i \in \bar{v}} s_i \quad (26)$$

associated with some vertex set  $\bar{v}$ . By equation (22) it is apparent this can be written as:

$$s_{\bar{v}} = \left( \prod_{i \in \bar{v}} X_i \right) \exp(i\pi e_{\bar{v}} R), \quad (27)$$



where  $R$  is some  $e_{\bar{v}}$ -independent multilinear degree- $k$  polynomial in the  $\frac{I-Z_i}{2}$  with integer coefficients. As the commutation in equation (22) only introduces terms of up to a single degree lower than the commuted  $U_{\bar{v}}$ , we can also calculate the constant term  $R_0$  in  $R$ :

$$R_0 = 1. \quad (28)$$

In particular,

$$\exp(i\pi e_{\bar{v}} R) |0\rangle^{\otimes n} = \exp(i\pi e_{\bar{v}}) |0\rangle^{\otimes n}. \quad (29)$$

Similarly, by equation (21)

$$s_{\bar{v}} = \exp(i\pi e_{\bar{v}} L) \prod_{i \in \bar{v}} X_i, \quad (30)$$

where once again  $L$  is some  $e_{\bar{v}}$ -independent multilinear degree- $k$  polynomial in the  $\frac{I-Z_i}{2}$ . By the Hermiticity of  $s_{\bar{v}}$  we must have that:

$$L = -R. \quad (31)$$

In particular, when  $e_{\bar{v}}$  is an integer, we have by equating these expressions for  $s_{\bar{v}}$  that:

$$\left[ \cos(\pi e_{\bar{v}}(R-1)), \prod_{i \in \bar{v}} X_i \right] = \mathbf{0}, \quad (32)$$

where:

$$\cos(\pi e_{\bar{v}}(R-1)) |0\rangle^{\otimes n} = |0\rangle^{\otimes n}. \quad (33)$$

## A.2 Qumode Weighted Hypergraph States

One can consider a qumode version of  $k$ -uniform weighted hypergraph states completely analogously to qubit weighted hypergraph states (Takeuchi et al., 2019). The standard definition of such states involves the sequential application of qumode multi-controlled phase operators associated with a  $k$ -uniform hypergraph  $G$  on a momentum-squeezed state:

$$|G\rangle \equiv \prod_{\bar{v} \in G} \exp\left(i e_{\bar{v}} \prod_{j \in \bar{v}} \hat{q}_j\right) |\mathbf{0}\rangle_{\hat{p}}. \quad (34)$$

We modify this definition slightly for our purposes; we consider an initial *GKP state* (Gottesman et al., 2001):

$$|\text{GKP}\rangle \propto \bigotimes_{i=1}^n \left( \sum_{\alpha=-\infty}^{\infty} |\alpha\rangle_{\hat{q}_i} \right). \quad (35)$$

Specifically, we take *qumode  $k$ -uniform weighted hypergraph states* associated with a  $k$ -uniform hypergraph  $G$  to be defined as:

$$|G\rangle \equiv \prod_{\bar{v} \in G} U_{\bar{v}}(e_{\bar{v}}) |\text{GKP}\rangle, \quad (36)$$

where now in a qumode context we have defined:

$$U_{\bar{v}}(e_{\bar{v}}) \equiv \exp\left(i\pi e_{\bar{v}} \prod_{j \in \bar{v}} \hat{q}_j\right). \quad (37)$$

It is once again easy to check the commutation relations when  $i \in \bar{v}$ :

$$X_i U_{\bar{v}}(e_{\bar{v}}) = U_{\bar{v} \setminus \{i\}}(-e_{\bar{v}}) U_{\bar{v}}(e_{\bar{v}}) X_i, \quad (38)$$

$$U_{\bar{v}}(e_{\bar{v}}) X_i = X_i U_{\bar{v} \setminus \{i\}}(e_{\bar{v}}) U_{\bar{v}}(e_{\bar{v}}), \quad (39)$$

where now:

$$X_i \equiv \exp(-2i\hat{p}_i). \quad (40)$$

Similarly to qubit  $k$ -uniform weighted hypergraph states, the qumode version of these states are described by commuting stabilizers:

$$\begin{aligned} s_i &= \prod_{\bar{v} \ni i} U_{\bar{v}}(e_{\bar{v}}) X_i \left( \prod_{\bar{v} \ni i} U_{\bar{v}}(e_{\bar{v}}) \right)^\dagger \\ &= X_i \prod_{\bar{v} \ni i} U_{\bar{v} \setminus \{i\}}(e_{\bar{v}}) \end{aligned} \quad (41)$$

and their Hermitian conjugates. Unlike the qubit case, however, the  $s_i$  are now not Hermitian.

We now consider the special case where  $G$  has only a single hyperedge  $\bar{v}$ . Consider the stabilizer of  $|G\rangle$ :

$$s_{\bar{v}} \equiv \prod_{i \in \bar{v}} s_i \quad (42)$$

associated with some vertex set  $\bar{v}$ . By equation (39) it is apparent this can be written as:

$$s_{\bar{v}} = \left( \prod_{i \in \bar{v}} X_i \right) \exp(i\pi e_{\bar{v}} R), \quad (43)$$

where  $R$  is some  $e_{\bar{v}}$ -independent multilinear degree- $(k-1)$  polynomial in the  $\hat{q}_i$  with integer coefficients. As the commutation in equation (39) only introduces terms of up to a single degree lower than the commuted  $U_{\bar{v}}$ , we can also calculate the constant term  $R_0$  in  $R$ :

$$R_0 = 1. \quad (44)$$

In particular,

$$\exp(i\pi e_{\bar{v}} R) |\mathbf{0}\rangle_{\hat{q}} = \exp(i\pi e_{\bar{v}}) |\mathbf{0}\rangle_{\hat{q}}. \quad (45)$$

Unlike the qubit case, the  $s_{\bar{v}}$  are now *not* Hermitian, and particular it is not true that  $\exp(i\pi e_{\bar{v}} R)$  commutes through  $\prod_{i \in \bar{v}} X_i$  up to conjugation. However, this *is* true up to stabilizers of  $|G\rangle$  when  $e_{\bar{v}}$  is an integer. Namely, using equation (39) we have that:

$$\exp(i\pi e_{\bar{v}} R) \left( \prod_{i \in \bar{v}} X_i \right) = \left( \prod_{i \in \bar{v}} X_i \right) \exp(i\pi e_{\bar{v}} R) \exp(2i\pi e_{\bar{v}} \tilde{R}), \quad (46)$$

where  $\tilde{R}$  is another  $e_{\bar{v}}$ -independent multilinear degree- $k$  polynomial in the  $\hat{q}_i$  with integer coefficients and no constant term. As  $\exp(2i\pi e_{\bar{v}} \tilde{R})$  commutes with  $U_{\bar{v}}(e_{\bar{v}})$  and as  $|G\rangle$  is a uniform superposition state over squeezed integer positions,

$$\exp(i\pi e_{\bar{v}} R) \left( \prod_{i \in \bar{v}} X_i \right) |G\rangle = \left( \prod_{i \in \bar{v}} X_i \right) \exp(i\pi e_{\bar{v}} R) |G\rangle. \quad (47)$$

This is similar to an idea used in the work of Wan et al. (2021), where generated high-weight errors in a proposed fault-tolerant quantum computing scheme were shown to be equivalent to low-weight errors up to stabilizers. We thus have when  $e_{\bar{v}}$  is an integer that for all integer  $\alpha$ :

$$\left[ \exp(i\alpha\pi e_{\bar{v}} (R-1)), \prod_{i \in \bar{v}} X_i \right] |G\rangle = \mathbf{0}, \quad (48)$$

where:

$$\exp(i\pi e_{\bar{v}} (R-1)) |\mathbf{0}\rangle_{\hat{q}} = |\mathbf{0}\rangle_{\hat{q}}. \quad (49)$$

As the projector onto the  $\exp(i\pi e_{\bar{v}} (R-1)) = 1$  subspace can be written as integer powers of  $\exp(i\pi e_{\bar{v}} (R-1))$ , this implies that the measurement (given this measurement outcome) commutes with the product of vertex stabilizers of  $|G\rangle$ .

## B Informal Discussion of the Qubit-Based Construction

We here discuss a qubit-based analog of the qumode construction of  $k$ -HRNNs and the  $(\ell, n, k)$ -HSMT task discussed in the main text, following the structure of Sections 3 and 4. Our presentation here will be of the same level of rigor as the main text for ease of reading, with more rigorous definitions and constructions given in Appendices A and C.

### B.1 Qubit $k$ -HRNNs

We consider a similar construction for qubit  $k$ -HRNNs as the CV version introduced in Section 3. As this model now acts on a finite-dimensional Hilbert space, we no longer motivate it as the quantization of a classical RNN. Furthermore, unlike the qumode model, the qubit model requires some specific constraints on its parameters for it to be trainable per the discussion of Section 2.3. We make two assumptions that will aid us in demonstrating this.

First, we demote the previously quantum input space  $\mathcal{M}$  to a classical input space as discussed in Section 3. The “parameters”  $\gamma, \theta$  in what follows should be considered trainable functions of the model inputs.

Second, our model will no longer be time invariant. Namely, for each time step through some predetermined time step  $\tau_1$ , a unitary  $U = \exp(-i\hat{G})$  is applied on the joint space indexed by  $\mathcal{N} \times \mathcal{O}$ :

$$\hat{G} = \sum_{c \in \mathcal{O}} \frac{I - X_c}{2} \otimes O_{\gamma_c, \theta_c}. \quad (50)$$

Here,

$$O_{\gamma_c, \theta_c} = \sum_{b \in \mathcal{N}} \gamma_{c,b} X_b \prod_{\bar{j} \in C_{\mathcal{N},k}} U_{\bar{j} \setminus \{b\}}(\theta_{c,\bar{j}}) U_{\bar{j}}(-2\theta_{c,\bar{j}}), \quad (51)$$

where:

$$U_{\bar{v}}(e_{\bar{v}}) \equiv \exp\left(i\pi e_{\bar{v}} \prod_{i \in \bar{v}} \frac{I - Z_i}{2}\right) \quad (52)$$

and  $C_{\mathcal{A},k}$  is the set of multisets indexing all subsets of cardinality at most  $k$  of indices with indices in  $\mathcal{A}$ .

Beginning at time step  $\tau_1 + 1$ , a different unitary  $V = \exp(-i\hat{H})$  is applied on the joint space indexed by  $\mathcal{N} \times \mathcal{O}$ :

$$\hat{H} = \sum_{c \in \mathcal{O}} \frac{I - X_c}{2} \otimes D_{\phi_c}. \quad (53)$$

Here,

$$D_{\phi_c} = \prod_{\bar{j} \in C_{\mathcal{N},k}} \frac{1}{2} \left( U_{\bar{j}}(\phi_{c,\bar{j}}) + U_{\bar{j}}(\phi_{c,\bar{j}})^\dagger \right), \quad (54)$$

where the  $\phi$  are not trained. Finally, beginning at time step  $\tau_2$ , unitary operators of the form of  $U$  are once again applied on the joint space indexed by  $\mathcal{N} \times \mathcal{O}$ .

Though this seems complex, the qubit  $k$ -HRNN is constructed in such a way to allow for the sequential measurement of qubit  $k$ -uniform hypergraph state stabilizers as reviewed in Appendix A.1, followed (beginning at time step  $\tau_1 + 1$ ) by the measurement of certain diagonal operators that are fixed functions of the input sequence, followed by final stabilizer measurements beginning at time step  $\tau_2 + 1$ .

We now introduce constraints on the  $\theta_c$  such that the resulting model is efficiently trainable. We first require that the first  $\tau_1$   $O_{\gamma_c, \theta_c}$  correspond to (weighted sums of) stabilizers of some qubit weighted hypergraph state; if this were not the case, it is easy to see that the Lie bracket could propagate  $X_b$  operators to multiple qubits, yielding an exponential dynamical Lie algebra dimension. This trivially does not happen if they indeed correspond to the stabilizers of some fixed state as then, of course, all of the  $O_{\gamma_c, \theta_c}$  will commute. This also implies that, just as for the qumode HRNN, each unit cell is a member of  $\text{QNC}_{\text{wf}}^0$ .

For simplicity, we assume further that  $\tau_1 \geq n$  and that the  $O_{\gamma_c, \theta_c}$  are chosen to yield a hypergraph state  $|G\rangle$  on  $n$  qubits (rather than potentially on some subset of  $n$  qubits, or one of another class of states if they were linearly dependent). We also assume that  $\tau_2 - \tau_1 \geq n - k$ , and that  $n - k$  of these measurements are single qubit measurements of Pauli  $Z$  operators on distinct qubits. Note that by construction (i.e., as the initial state is a qubit hypergraph state) these measurement statistics are always uniform over  $\pm 1$ . Furthermore, with classically-controlled diagonal operators, any diagonal operators associated with the measured qubit can be removed from the hypergraph state. These classically-controlled operators depend on the hypergraph state itself, and we thus once again emphasize that our results do not demonstrate a quantum-classical separation during training, just inference; this is further discussed in Appendix E.3. The resulting state is effectively then an induced  $k$ -qubit hypergraph state. For constant  $k$ , any further operations applied to the resulting state during the training procedure is efficient by the discussion in Section 2.3. We note that the formal version of the learning task described in Appendix C.1.1 along with the antidistinguishing measurement sequences described in Lemma C.1 which we use to prove our quantum-classical separations fit into this framework.

An intuitive way to think about this learning scenario is as a learning algorithm tasked with finding a mapping from inputs to hypergraph states—which is an  $\sim n^k$ -dimensional manifold—choosing a  $k$ -vertex subhypergraph depending on the inputs, and then performing operations on some  $k$ -qubit state dependent on this subhypergraph. As the accessible state space grows only polynomially with  $n$ , training times also scale only polynomially with  $n$ .

## B.2 Qubit $(\ell, n, k)$ -HSMT

For qubit  $(\ell, n, k)$ -HSMT (where  $\ell \geq 2n - k$ ) we consider input sequences composed of classical descriptions of qubit  $k$ -uniform hypergraph state stabilizer generators:

$$s_b = X_b \prod_{\bar{j} \in \mathcal{C}_{\mathcal{N}, k}} U_{\bar{j} \setminus \{b\}}(\theta_{c, \bar{j}}) U_{\bar{j}}(-2\theta_{c, \bar{j}}) \quad (55)$$

on some  $n$ -qubit space indexed by  $\mathcal{N}$  for  $n$  time steps, where every  $b \in \mathcal{N}$  is measured at least once. The task is such that the  $s_b$  are guaranteed to commute; this is to ensure the trainability of the associated qubit  $k$ -HRNN, as described in Appendix B.1. For time steps  $n + 1$  through  $2n - k$ , the  $(\ell, n, k)$ -HSMT is composed of classical descriptions of Pauli  $Z$  operators:

$$d_b = Z_b, \quad (56)$$

where once again each  $b \in \mathcal{N}$  is unique. Finally, for time steps  $2n - k + 1$  through  $\ell$ , measurements are of operators composed of products of those described in equation (55) on the  $k$  qubits indexed by  $\mathcal{N}$  not measured in the previous step.

Just as in the qumode  $(\ell, n, k)$ -HSMT, the qubit  $(\ell, n, k)$ -HSMT is defined such that a translation  $\mathbf{y}$  of  $\mathbf{x}$  is considered correct if it describes measurement results consistent with measuring observables described by  $\mathbf{x}$  when beginning in the computational basis state  $|0\rangle^{\otimes n}$ . By construction, the qubit  $k$ -HRNN can perform qubit  $(\ell, n, k)$ -HSMT to zero error with  $n$  qubits of memory using unit cells in QNC<sub>wf</sub><sup>0</sup> (Moore & Nilsson, 2001; 1998; Høyer & Špalek, 2005).

# C Proofs of Expressivity Separations

## C.1 $(\ell, n, k)$ -Hypergraph Stabilizer Measurement Translation

Before giving proofs of expressivity separations between our quantum model and classical models, we first give a formal definition of the translation task we will prove a separation on: namely,  $(\ell, n, k)$ -hypergraph stabilizer measurement translation ( $(\ell, n, k)$ -HSMT), parameterized by  $\ell$ ,  $n$ , and  $k$ , where  $\ell \geq 2n$ . Note that the technical description of the task described here slightly differs from construction presented in the main text. As the construction of the task differs slightly from what was presented in the main text, so

must the constructions of  $k$ -hypergraph recurrent neural networks ( $k$ -HRNNs) differ slightly from what was described in Section 3. However, the required changes follow straightforwardly from the formal statement of  $(\ell, n, k)$ -HSMT and do not change any of our conclusions, so we will leave these changes implicit.

We give a version of the task more natural for qubit-based systems, and a version more natural for qumode-based systems.

### C.1.1 Qubit $(\ell, n, k)$ -HSMT

Let  $\boldsymbol{\theta}$  be the  $n \left(1 + \binom{n-1}{k-1}\right) + \binom{n}{k}$ -dimensional vector describing the operator:

$$O_{\boldsymbol{\theta}} = \sum_{i=1}^n \left( \theta_{i,X} X_i \prod_{\bar{v} \ni i; |\bar{v}|=k} U_{\bar{v} \setminus \{i\}}(-\theta_{\bar{v}}) U_{\bar{v}}(2\theta_{\bar{v}}) - \theta_{i,X} \right) + \prod_{|\bar{w}| \leq k} \frac{1}{2} \left( U_{\bar{w}}(\theta_{\bar{w},Z}) + U_{\bar{w}}(\theta_{\bar{w},Z})^\dagger \right). \quad (57)$$

Here,  $U_{\bar{v}}(\alpha)$  is the  $\alpha$ th power of a  $C^k Z_{\bar{v}}$  operator, as defined in equation (19). This is a Hermitian observable by equation (23). We consider an input language given by  $\ell$ -long sequences of these words. Specifically, input sentences are composed of words:

$$\boldsymbol{x} = \left( \boldsymbol{\theta}^{(1)}, \dots, \boldsymbol{\theta}^{(\ell)} \right)^\top. \quad (58)$$

The first  $n$  rows of  $\boldsymbol{x}$  describe the sequential measurement of each operator  $\exp(iO_{\boldsymbol{\theta}})$  when beginning in  $|0\rangle^{\otimes n}$  via, e.g., phase estimation (Nielsen & Chuang, 2010). The next  $n$  words query the model to reproduce the measurement result outputted  $n$  measurements prior; we require this repetition of outputs for technical reasons for the autoregressive separations, though do not require it for the encoder-decoder separations (and call this scenario hypergraph stabilizer measurement translation *without repetition*). The final  $\ell - 2n$  (or  $\ell - n$  without repetition) rows return to describing the sequential measurement of each operator  $\exp(iO_{\boldsymbol{\theta}})$ .

A translation  $\boldsymbol{y}$  of  $\boldsymbol{x}$  is considered correct if it is of the form

$$\boldsymbol{y} = (m_1, \dots, m_n, m_1, \dots, m_n, m_{\ell-2n+1}, \dots, m_\ell)^\top, \quad (59)$$

where the measurement outcomes  $m_i$  are consistent with those of quantum mechanics. To prove our separations, we will consider input sentences that exhibit quantum contextuality. Note that a qubit  $k$ -HRNN can perform this task perfectly via phase estimation (Nielsen & Chuang, 2010).

### C.1.2 Qumode $(\ell, n, k)$ -HSMT

For technical reasons, the exact description of the qumode HSMT task differs slightly than that of the qubit version. We define the parameterized operators:

$$O_{\boldsymbol{\theta}}^i = \exp(2i\theta_{i,p}\hat{p}_i), \quad (60)$$

$$V_{\boldsymbol{\theta}}^i = \exp\left(i \sum_{\bar{v} \ni i} \theta_{\bar{v}} \hat{q}_{\bar{v}}\right), \quad (61)$$

$$W_{\boldsymbol{\theta}} = \exp\left(i \sum_{i=1}^n \left( \theta_{i,p} \hat{p}_i + \theta_{i,q} \hat{q}_i + \sum_{\bar{j} \in \tilde{C}_{k-1,i}} \theta_{i,\bar{j}} \hat{q}_{\bar{j}} \right)\right). \quad (62)$$

We consider an input language given by  $\ell$ -long sequences of words:

$$\boldsymbol{x} = \left( \boldsymbol{\theta}^{(1)}, \dots, \boldsymbol{\theta}^{(\ell)} \right)^\top. \quad (63)$$

The first  $n$  rows of  $\boldsymbol{x}$  describe the sequential measurement of each operator  $O_{\boldsymbol{\theta}}^i$  when beginning in the position-squeezed state  $|0\rangle_{\hat{q}}$ . When  $\theta_{i,p} = 1$  and the measurement outcomes are  $+1$ , this sequence of

measurements projects onto the GKP state described in equation (35); this can be seen by considering the phase estimation circuit (Liu et al., 2016) measuring  $O_{\theta_{i,p}}$  in the position basis, and considering its action on the state  $|0\rangle_{\hat{q}_i}$ .

The second  $n$  rows describe the sequential *application* of each operator  $V_{\theta}^i$  on the post-measurement state.

The third  $n$  rows query the model to reproduce the first  $n$  measurement results (or are excluded, if we are studying hypergraph stabilizer measurement *without repetition*).

Finally, the final  $\ell - 3n$  (or  $\ell - 2n$  without repetition) rows describe the sequential measurement of each operator  $W_{\theta}$ .

The maximum dimension of a given  $\theta$  describing an operator throughout the entire task is  $W_{\theta}$ , where it is of dimension:

$$m = n \left( 2 + \binom{n-1}{k-1} \right). \quad (64)$$

We assume for simplicity that in other stages of the translation task, the parameters are padded to be of this length.

A translation  $\mathbf{y}$  of  $\mathbf{x}$  is considered correct if it is of the form:

$$\mathbf{y} = (m_1, \dots, m_n, 0, \dots, 0, m_1, \dots, m_n, m_{\ell-3n+1}, \dots, m_{\ell})^{\top}, \quad (65)$$

where the measurement outcomes  $m_i$  are consistent with those of quantum mechanics given the previously described procedure. To prove our separations, we will consider input sentences that exhibit prepare non-Gaussian states in the quantum system they describe; equivalently, they exhibit quantum contextuality (Booth et al., 2022). Note that a qumode  $k$ -HRNN can perform this task perfectly via phase estimation (Liu et al., 2016).

## C.2 Single-copy Antidistinguishing Measurement Sequences via Quantum Contextuality

We now prove two lemmas demonstrating the existence of *antidistinguishing measurement sequences* given by qubit  $k$ -uniform weighted hypergraph state stabilizers, as well as qumode  $k$ -uniform hypergraph state stabilizers. Antidistinguishing measurement sequences are those which, given  $r$  candidates for a given quantum state, rule out one candidate with certainty (Leifer, 2014).

We first prove that antidistinguishing measurement sequences via the measurement of quantum contextual observables between qubit  $k$ -uniform hypergraph states exist.

**Lemma C.1** (Qubit  $k$ -uniform hypergraph states are antidistinguishable). *Consider the state  $|0\rangle^{\otimes n}$ . Let  $|\psi_1\rangle$  and  $|\psi_2\rangle$  be two qubit  $k$ -uniform weighted hypergraph states with a hyperedge differing by 1. There exists an antidistinguishing measurement sequence (via measuring quantum contextual observables of the form of equation (57)) of length  $n - k + 2$  that with certainty discounts one of the three states.*

*Proof.* Let  $\bar{v}$  be the set of vertices associated with a hyperedge where  $|\psi_1\rangle$  and  $|\psi_2\rangle$  have weights  $e'_{\bar{v}}, e''_{\bar{v}}$ , respectively, differing by 1. For simplicity, we consider the basis transformed by powers of  $C^k Z$  operations such that  $e'_{\bar{v}} = 0$  and  $e''_{\bar{v}} = 1$ ; note that this can be done without loss of generality (WLOG) as this basis transformation maps the class of operators described in equation (57) to itself, as well as maps  $|0\rangle^{\otimes n}$  to itself.

The antidistinguishing measurement sequence first consists of measuring  $Z_i$  for all qubits labeled by  $i$  associated with the  $n - k$  vertices not in  $\bar{v}$ ; if one of these measurement results is not 1, then  $|0\rangle^{\otimes n}$  is discounted (i.e., the state in question is known not to be  $|0\rangle^{\otimes n}$ ). We assume then that they are all 1. For all  $i \in \bar{v}$ , we have by definition that the post-measurement state of  $|\psi_1\rangle$  is then just:

$$|+\rangle^{\otimes n}, \quad (66)$$

and the post-measurement state of  $|\psi_2\rangle$  just the unweighted qubit graph state with stabilizers:

$$s_i = X_i C^k Z_{\bar{v} \setminus \{i\}}. \quad (67)$$

Consider now the measurement of the operator:

$$M = \cos(\pi(R-1)), \quad (68)$$

where  $R$  is defined as in equation (27). As  $\exp(i\pi(R-1))$  is a product of multi-controlled  $Z$  operators, and as multi-controlled  $Z$  operators are Hermitian,  $M$  can be written as a product of multi-controlled  $Z$  operators.

By the discussion surrounding equation (27),  $R-1$  nullifies  $|0\rangle^{\otimes n}$ . Thus, the measurement result of  $M$  must be  $+1$ ; otherwise,  $|0\rangle^{\otimes n}$  would be distinguished. Furthermore, from equation (32), this measurement commutes with the product of vertex stabilizers for  $|\psi_1\rangle, |\psi_2\rangle$ . Note also that the projection onto the subspace where  $M=1$  is equal to the projection onto the subspace where  $\exp(i\pi(R-1))=1$ . Thus, the post-measurement states  $|\phi_1\rangle, |\phi_2\rangle$  of  $|\psi_1\rangle, |\psi_2\rangle$ , respectively, then are respectively stabilized by:

$$t' = \prod_{i \in \bar{v}} X_i, \quad (69)$$

$$t'' = - \prod_{i \in \bar{v}} X_i. \quad (70)$$

$|\phi_1\rangle$  and  $|\phi_2\rangle$  are thus orthogonal with distinguishing measurement given by  $t'$ .  $\square$

The antidistinguishing measurement sequence for qumodes is similar.

**Lemma C.2** (Qumode  $k$ -uniform hypergraph states are antidistinguishable). *Consider the state  $|\mathbf{0}\rangle_{\hat{q}}$ . Let  $|\psi_1\rangle$  and  $|\psi_2\rangle$  be two qumode  $k$ -uniform weighted hypergraph states with a hyperedge differing by 1. There exists an antidistinguishing measurement sequence (via measuring quantum contextual observables of the form of equation (62)) of length  $n-k+2$  that with certainty discounts one of the three states.*

*Proof.* Let  $\bar{v}$  be the set of vertices associated with a hyperedge where  $|\psi_1\rangle$  and  $|\psi_2\rangle$  have weights  $e'_{\bar{v}}, e''_{\bar{v}}$ , respectively, differing by 1. We assume WLOG that  $e''_{\bar{v}} < e'_{\bar{v}}$ ; note that we cannot assume WLOG anymore that one is 0 and the other 1, as the class of operators described in equation (60) no longer maps to itself under conjugation by the required basis transformation.

The antidistinguishing measurement sequence first consists of measuring  $\hat{q}_i$  for all qubits labeled by  $i$  associated with the  $n-k$  vertices not in  $\bar{v}$ ; if one of these measurement results is not 0, then  $|\mathbf{0}\rangle_{\hat{q}}$  is discounted (i.e., the state in question is known not to be  $|\mathbf{0}\rangle_{\hat{q}}$ ). We assume then that they are all 0. For all  $i \in \bar{v}$ , we have by definition that the post-measurement state of  $|\psi_1\rangle$  is then just the  $k$ -uniform weighted qumode graph state with stabilizers::

$$s'_i = X_i \exp\left(i\pi e'_{\bar{v}} \prod_{j \in \bar{v}} \hat{q}_j\right), \quad (71)$$

and the post-measurement state of  $|\psi_2\rangle$  just the unweighted qumode graph state with stabilizers:

$$s''_i = X_i \exp\left(i\pi e''_{\bar{v}} \prod_{j \in \bar{v}} \hat{q}_j\right). \quad (72)$$

Consider now the measurement of the operator:

$$M = \exp(i\pi(R-1)), \quad (73)$$

where  $R$  is defined as in equation (43).

By the discussion surrounding equation (27),  $\exp(i\pi(R-1))$  stabilizes  $|\mathbf{0}\rangle_{\hat{q}}$ . Thus, the measurement result of  $M$  must be  $+1$ ; otherwise,  $|\mathbf{0}\rangle_{\hat{q}}$  would be distinguished. Furthermore, from equation (48), this measurement commutes with the product of vertex stabilizers for  $|\psi_1\rangle, |\psi_2\rangle$ , up to stabilizers of  $|\psi_1\rangle, |\psi_2\rangle$ . Thus, the post-measurement states  $|\phi_1\rangle, |\phi_2\rangle$  of  $|\psi_1\rangle, |\psi_2\rangle$ , respectively, then are respectively stabilized by:

$$t' = s', \quad (74)$$

$$t'' = \exp(i\pi(e''_{\bar{v}} - e'_{\bar{v}})) s' = -s'. \quad (75)$$

$|\phi_1\rangle$  and  $|\phi_2\rangle$  are thus orthogonal with distinguishing measurement given by  $t'$ .  $\square$

### C.3 Expressivity Separation for Autoregressive Models

We consider now an autoregressive learner with structure given by Figure 1(a). We assume for simplicity that the learner is deterministic after given a random vector  $\mathbf{r}$ . This class of models includes implementations of stochastic simulation algorithms such as Wigner function simulation (Mari & Eisert, 2012) as well as generative adversarial networks (GANs) (Goodfellow et al., 2014). As for each  $\mathbf{r}$ , we will demonstrate that there exists an input sequence such that any classical model with  $\dim(L) < \binom{n}{k} - 1$  deterministically outputs a measurement sequence inconsistent with quantum mechanics, our results will still hold when considering the model over its randomness. Due to this we will often take the  $\mathbf{r}$ -dependence to be implicit.

Autoregressive neural sequence models at time step  $i$  map an  $m$ -dimensional input token  $\mathbf{x}_i$  and a latent vector  $\boldsymbol{\lambda}_{i-1}$  to an output token  $m_i$  and a new latent vector  $\boldsymbol{\lambda}_i$ . After  $n$  steps (or  $2n$ , in the case of the qumode separation), then, we can consider the autoregressive model as a function:

$$\mathcal{F}^{\mathbf{r}} : (\mathbb{R}^m)^n \rightarrow L \times \mathbb{R}^n \quad (76)$$

where  $\mathbf{r}$  is a random vector such that, for any  $\mathbf{r}$ ,  $\mathcal{F}^{\mathbf{r}}$  is deterministic. In the following we will assume that  $L$  is a  $C^2$  contractible Finsler manifold; concrete examples of such a manifold are the open ball  $L = (0, 1)^d$  and the reals  $L = \mathbb{R}^d$  for some  $d = \dim(L)$ .

We now state our conditions on  $\mathcal{F}^{\mathbf{r}}$ . Our proofs of Theorems C.3 and C.4 concern a subspace  $K$  of inputs corresponding to measurements of hypergraph state stabilizers. We require that the projection of  $\mathcal{F}^{\mathbf{r}}$  onto  $L$  is  $C^2$  on a contractible,  $(\dim(L) + 2)$ -dimensional, open subset  $U \subseteq K$ . As  $\dim(K) = \binom{n}{k}$ , our assumption on the dimension of  $U$  is satisfied when  $U$  is not measure zero in  $K$  and  $L < \binom{n}{k} - 1$ , as stated in the main text. We also require that on  $U$ ,  $\mathcal{F}^{\mathbf{r}}$  is a *strong submersion* (Rabier, 1997)—namely,  $U$  is such that the Jacobian of  $\mathcal{F}^{\mathbf{r}}$  has a  $\dim(L) \times \dim(L)$  minor with lower-bounded determinant. This is effectively a requirement that the model is *strongly Morse* (Mokhtari et al., 2019) in a multivariate sense. Neural networks being strongly Morse (in the univariate case) is a common assumption (Mei et al., 2018; Mokhtari et al., 2019; Yang et al., 2021; Dixit et al., 2023), and certain classes of neural networks are known to be almost surely Morse over settings of their parameters (Kurochkin, 2021). Finally, we require as a technical assumption that no sequence with limit point in  $\partial U \not\subseteq U$  maps to a sequence with limit point in  $L$  under  $\mathcal{F}^{\mathbf{r}}$  (projected onto  $L$ ). By the “global implicit function theorem” of Rabier (1997),  $\mathcal{F}^{\mathbf{r}}$  (projected onto  $L$ ) is then “globally” (on  $U$ ) a trivial bundle with base space  $C^1$ -diffeomorphic to  $L$ . This, along with Lemmas C.1 and C.2, are the central implications which we will use to prove our theorems.

We give three simple examples that immediately imply our strong submersion condition on (an assumed  $C^2$ )  $\mathcal{F}^{\mathbf{r}}$ :

1. The presence of an appropriate  $\ell_2$  regularization term dominating at infinity.
2. More generally, assuming that updates to the model during training (via, for instance, gradient descent) are bounded, as our conditions are implied by regularity of the model at infinity. A similar approach was taken in the work of Shi et al. (2020) in justifying certain regularity conditions of machine learning models at infinity.
3. The model is implemented at a finite precision  $\epsilon \ll 1$ . A critical value, by definition, has at least one local coordinate that varies only by  $\sim \epsilon^2 \approx 0$  for an  $\epsilon$ -perturbation of a critical point. This locally-constant (at precision  $\epsilon$ ) set of local coordinates can be projected out, then, yielding an equivalent model with maximal-rank Jacobian in the neighborhood of this point (with lower-bounded associated minor determinant), with effective latent space  $\tilde{L}$  of lower dimension than  $L$ .

We give two simple examples that imply our condition on certain limit points not existing in  $L$ :

1.  $U$  does not contain a boundary at all, e.g., a sufficiently strong regularity condition is imposed on  $\mathcal{F}^{\mathbf{r}}$  such that it is a strong submersion on an unbounded subspace. This is similar to the first two examples previously mentioned.



2.  $\mathcal{F}^r$  is a proper open map (onto its image) on  $U \cup \partial U$ , such as if it is composed of linear transformations and leaky rectified linear units. This is as under such a map,  $\partial U$  maps to  $\partial(\mathcal{F}^r(U))$ , which has no intersection with  $\mathcal{F}^r(U)$  as  $\mathcal{F}^r$  is open. To see this, assume some point  $d \in \partial U$  mapped to  $y \in \mathcal{F}^r(U)$ . By the definition of this set, there must also be some  $u \in U$  mapping to  $y$  under  $\mathcal{F}^r(U)$ . As  $\mathcal{F}^r(U)$  is proper, there must be a neighborhood of  $y$  with preimage (intersected with  $U$ ) compactly contained in  $U$ . However, the image of any Cauchy sequence  $(x_i)$  in  $U$  approaching  $d \notin U$  must be in this neighborhood of  $y$  for sufficiently large  $i$  by continuity, violating compactness and yielding a contradiction.

### C.3.1 Qubit Separation

With the preliminaries in place, we now prove our expressivity separation on the qubit-based task.

**Theorem C.3** (Autoregressive qubit hypergraph stabilizer measurement translation memory lower bound). *Consider an autoregressive model with  $C^2$  contractible Finsler latent manifold  $L$ , and model function after  $n$  steps*

$$\mathcal{F} : \mathbb{R}^{mn} \rightarrow L \times \mathbb{R}^n. \quad (77)$$

*Assume that the projection of  $\mathcal{F}$  onto  $L$  is  $C^2$  on a contractible, open subset  $U \subseteq K$ , where  $U$  is a  $C^1$  manifold of dimension at least  $\dim(L) + 2$  and where  $K \subset \mathbb{R}^{mn}$  is as described in equation (79). Assume also that  $\mathcal{F}$  is a strong submersion on  $U$ , and that no sequence with limit point in  $\partial U \not\subseteq U$  maps to a sequence with limit point in  $L$  under  $\mathcal{F}$  projected onto  $L$ .*

*This model cannot achieve a finite backward empirical cross entropy on the qubit  $(3n - k + 2, n, k)$ -hypergraph stabilizer measurement translation task due to quantum contextuality.*

*Proof.* Let

$$m = n \left( 1 + \binom{n-1}{k-1} \right) + \binom{n}{k} \quad (78)$$

be the dimension of each row of an input sentence to the model. Consider  $K \subset (\mathbb{R}^m)^n$ , the space of the first  $n$  rows of input sentences with elements of the form:

$$\mathbf{Q} = \left( \boldsymbol{\theta}^{(1)}, \dots, \boldsymbol{\theta}^{(n)} \right)^\top, \quad (79)$$

where:

1. All  $\theta_{\bar{w}, Z}^{(a)}$  are 0.
2. All  $\theta_{\bar{v}}^{(a)}$  with  $a \notin \bar{v}$  are  $\mathbf{0}$ .
3.  $\theta_{\bar{v}}^{(i)}$  are the nonzero entries of a valid (potentially trivial) rank- $k$  adjacency tensor  $\mathbf{A}$  of a  $k$ -uniform hypergraph; that is, it is invariant under permutations of the indices.
4. All  $\theta_{i, X}^{(i)}$  are equal to the squared sum of entries of  $\mathbf{A}$ , i.e., its Frobenius norm.

Due to the bijection between  $\mathbf{Q} \in K$  and the associated hypergraph adjacency tensor  $\mathbf{A}$ , we will often use  $\mathbf{A}$  to refer to its associated  $\mathbf{Q}$  by proxy.

It is obvious from this construction that  $K$  is an  $\binom{n}{k}$ -dimensional embedding of representations of  $k$ -uniform hypergraphs via their adjacency tensors. Thus, the states described by the measurement scenarios of nontrivial points in  $K$  are exactly qubit  $k$ -uniform weighted hypergraph states with, depending on the measurement results, perhaps overall phases on the stabilizers.

We will proceed as follows. First, we will show that when  $\dim(L)$  is sufficiently small,  $\mathcal{F}$  must map three distinct qubit  $k$ -uniform hypergraph states described by different  $\mathbf{Q}$  to the same point in latent space. The next  $n$  outputs ensure that the previous measurement results of states mapped to the same point must be identical for the output translation to be correct. Then, we will use Lemma C.1 to show that the stabilizers of these states give rise to an antidistinguishing measurement sequence of length  $n - k + 2$  once the phases on their

stabilizers have been fixed to be identical. Thus, by considering measurement sequences of length  $3n - k + 2$  that include the position-squeezed state and these two  $k$ -uniform weighted hypergraph states, followed by the first  $n$  measurement results such that they are all fixed to be identical, and their antidistinguishing measurement sequence, one of the measurement outcomes must be incorrect. This implies that there is an infinite backward empirical cross entropy on any finite set containing these three measurement sequences.

We denote by  $\Pi_L \circ \mathcal{F}$  the projection of  $\mathcal{F}$  onto  $L$ . By Theorem 5.2 of Rabier (1997), following our assumptions,  $\Pi_L \circ \mathcal{F}|_U$  is a fiber bundle with base space  $C^1$ -diffeomorphic to  $L$  and induces a  $C^1$ -diffeomorphism  $\eta : H \times L \rightarrow U$ :

$$H \times L \cong U. \quad (80)$$

In particular,  $\Pi_L \circ \mathcal{F}|_U$  is a trivial bundle, and  $H$  is thus contractible and of dimension:

$$\dim(H) = \dim(U) - \dim(L) \geq 2. \quad (81)$$

We claim that  $\eta(H \times \{\lambda\})$  is unbounded for all  $\lambda \in L$ . To see this, first note that as  $\eta$  is a homeomorphism, the boundary of  $\eta(H \times \{\lambda\})$  for all  $\lambda \in L$  must be a subset of  $\partial U$ . Assume now that it is nonempty, i.e., that there existed a Cauchy sequence with limit point in  $\partial H \times \{\lambda\}$  that mapped to a Cauchy sequence with limit point in  $\partial U$  under  $\eta$ . Then, a sequence with limit point in  $\partial U$  would have base point  $\lambda \in L$ , violating our assumption that no sequence with limit point in the boundary of  $U$  has limit point in  $L$  under  $\Pi_L \circ \mathcal{F}$ . Thus,  $\eta(H \times \{\lambda\})$  has no boundary. In particular, as  $\eta(H \times \{\lambda\})$  is contractible, it is not compact as closed manifolds cannot be contractible. As  $\eta(H \times \{\lambda\}) \subset K$  has no boundary it is therefore unbounded.

Now fix  $\lambda \in L$ . As  $\eta(H \times \{\lambda\})$  is unbounded and path-connected, there exist points with arbitrary 2-norm modulo  $2\pi$  in  $\eta(H \times \{\lambda\})$ ; namely, there exists a point  $\mathbf{h}_0 \in H$  such that (mapped under  $\eta$ ):

$$\theta_{i,X}^{(i)} \equiv 0 \pmod{2\pi}. \quad (82)$$

This corresponds to trivial measurements in the translation task, fixing the measurement outcomes to all be  $+1$ . Note that  $\lambda$  is the image of  $\mathbf{h}_0$  under  $\Pi_L \circ \mathcal{F}$ . Assuming the model performs the translation task correctly, this fixes the measurement outcomes of the first  $n$  measurements to all be  $+1$  for *all* points mapping to  $\lambda$  under  $\Pi_L \circ \mathcal{F}$ , as the next  $n$  outputs are just recapitulations of these first  $n$  measurement outcomes and they must be consistent for all inputs mapping to  $\lambda$ .

Thus, there exists some coordinate  $\theta_* = \theta_v^{(i)}$  such that, for any sufficiently large  $\theta_*$ , there exists a point in  $K$  with this  $\theta_*$  that maps to  $\lambda$ . Furthermore, as  $H$  is of dimension at least 2, the 2-norm of the inputs can be assumed to be nonzero modulo  $2\pi$  by varying one of the other coordinates on  $\eta(H \times \{\lambda\})$ . Thus, there exist  $\mathbf{h}', \mathbf{h}'' \in U$  mapping to  $\lambda$  that describe qubit  $k$ -uniform weighted hypergraph states with some respective hyperedges  $e'_{\bar{v}}, e''_{\bar{v}}$  differing by 1.

By Lemma C.1, we have that there exists a measurement sequence (describable by the translation task) of length  $n - k + 2$  that antidistinguishes these three associated states with certainty. By then performing this antidistinguishing measurement sequence, the output for one of these  $\mathbf{h}_0, \mathbf{h}', \mathbf{h}''$  must then be incorrect. Thus, the model must obtain an infinite backward empirical cross entropy on these three sequences when followed by the antidistinguishing measurement sequence.  $\square$

### C.3.2 Qumode Separation

The separation for the qumode version of the hypergraph stabilizer measurement task proceeds similarly. For technical reasons, in the proof for the qumode separation we require the use of a periodic bump function, which we now define.

Consider the smooth transition function:

$$g(x) \equiv \left( \frac{\exp(-x^{-1})}{\exp(-x^{-1}) + \exp(-(1-x)^{-1})} \right). \quad (83)$$

The function

$$h_{a,b,c,d}(x) \equiv g\left(\frac{x-a}{b-a}\right)g\left(\frac{d-x}{d-c}\right) \quad (84)$$

is smooth, equal to 1 on the interval  $[b, c]$ , and vanishes outside of the interval  $(a, d)$ . The periodic bump function (the ‘‘bubble wrap’’ function):

$$t(x) \equiv \sum_{i=-\infty}^{\infty} h_{2\pi i, \frac{\pi}{2}+2\pi i, \pi+2\pi i, \frac{3\pi}{2}+2\pi i}(x) \quad (85)$$

is then a smooth function equal to 1 when  $x \equiv z \pmod{2\pi}$  for all  $\frac{\pi}{2} \leq z \leq \pi$ , and equal to 0 when  $x \equiv z \pmod{2\pi}$  for all  $\frac{3\pi}{2} \leq z \leq 2\pi$ .

**Theorem C.4** (Autoregressive qumode hypergraph stabilizer measurement translation memory lower bound). *Consider an autoregressive model with  $C^2$  contractible Finsler latent manifold  $L$ , and model function after  $2n$  steps*

$$\mathcal{F} : \mathbb{R}^{2mn} \rightarrow L \times \mathbb{R}^{2n}. \quad (86)$$

*Assume that the projection of  $\mathcal{F}$  onto  $L$  is  $C^2$  on a contractible, open subset  $U \subseteq K$ , where  $U$  is a  $C^1$  manifold of dimension at least  $\dim(L) + 2$  and where  $K \subset \mathbb{R}^{2mn}$  is as described in equation (88). Assume also that  $\mathcal{F}$  is a strong submersion on  $U$ , and that no sequence with limit point in  $\partial U \not\subseteq U$  maps to a sequence with limit point in  $L$  under  $\mathcal{F}$  projected onto  $L$ .*

*This model cannot achieve a finite backward empirical cross entropy on the qumode  $(4n - k + 2, n, k)$ -hypergraph stabilizer measurement translation task due to quantum contextuality.*

*Proof.* Let

$$m = n \left( 2 + \binom{n-1}{k-1} \right) \quad (87)$$

be the dimension of each row of an input sentence to the model. Consider  $K \subset (\mathbb{R}^m)^{2n}$ , the space of the first  $2n$  rows of input sentences with elements of the form:

$$\mathbf{Q} = \left( \boldsymbol{\theta}^{(1)}, \dots, \boldsymbol{\theta}^{(2n)} \right)^\top, \quad (88)$$

where:

1.  $\theta_v^{(i)}$  are the nonzero entries of a valid (potentially trivial) rank- $k$  adjacency tensor  $\mathbf{A}$  of a  $k$ -uniform hypergraph; that is, it is invariant under permutations of the indices.
2. All  $\theta_{i,p}^{(i)}$  are equal to the bump function  $t$  applied to the squared sum of entries of  $\mathbf{A}$ , i.e., its Frobenius norm.

Due to the bijection between  $\mathbf{Q} \in K$  and the associated hypergraph adjacency tensor  $\mathbf{A}$ , we will often use  $\mathbf{A}$  to refer to its associated  $\mathbf{Q}$  by proxy.

It is obvious from this construction that  $K$  is an  $\binom{n}{k}$ -dimensional embedding of representations of  $k$ -uniform hypergraphs via their adjacency tensors. Thus, if the first  $n$  measurement results are all  $+1$ , the states described by the measurement scenarios of nontrivial points in  $K$  are exactly qumode  $k$ -uniform weighted hypergraph states.

We will proceed as follows. First, we will show that when  $\dim(L)$  is sufficiently small,  $\mathcal{F}$  must map three distinct qumode  $k$ -uniform hypergraph states described by different  $\mathbf{Q}$  to the same point in latent space. The next  $n$  outputs ensure that the previous measurement results of states mapped to the same point must be identical for the output translation to be correct. Then, we will use Lemma C.2 to show that the stabilizers of these states give rise to an antidistinguishing measurement sequence of length  $n - k + 2$  once the phases on their stabilizers have been fixed to be identical. Thus, by considering measurement sequences of length  $4n - k + 2$  that include the position-squeezed state and these two  $k$ -uniform weighted hypergraph

states, followed by the first  $n$  measurement results such that they are all fixed to be identical, and their antidistinguishing measurement sequence, one of the measurement outcomes must be incorrect. This implies that there is an infinite backward empirical cross entropy on any finite set containing these three measurement sequences.

We denote by  $\Pi_L \circ \mathcal{F}$  the projection of  $\mathcal{F}$  onto  $L$ . By Theorem 5.2 of Rabier (1997), following our assumptions,  $\Pi_L \circ \mathcal{F}|_U$  is a fiber bundle with base space  $C^1$ -diffeomorphic to  $L$  and induces a  $C^1$ -diffeomorphism  $\eta : H \times L \rightarrow U$ :

$$H \times L \cong U; \tag{89}$$

in particular,  $\Pi_L \circ \mathcal{F}|_U$  is a trivial bundle, and  $H$  is thus path-connected and of dimension:

$$\dim(H) = \dim(U) - \dim(L) \geq 2. \tag{90}$$

We claim that  $\eta(H \times \{\lambda\})$  is unbounded for all  $\lambda \in L$ . To see this, first note that as  $\eta$  is a homeomorphism, the boundary of  $\eta(H \times \{\lambda\})$  for all  $\lambda \in L$  must be a subset of  $\partial U$ . Assume now that it is nonempty, i.e., that there existed a Cauchy sequence with limit point in  $\partial H \times \{\lambda\}$  that mapped to a Cauchy sequence with limit point in  $\partial U$  under  $\eta$ . Then, a sequence with limit point in  $\partial U$  would have base point  $\lambda \in L$ , violating our assumption that no sequence with limit point in the boundary of  $U$  has limit point in  $L$  under  $\Pi_L \circ \mathcal{F}$ . Thus,  $\eta(H \times \{\lambda\})$  has no boundary. In particular, as  $\eta(H \times \{\lambda\})$  is contractible, it is not compact as closed manifolds cannot be contractible. As  $\eta(H \times \{\lambda\}) \subset K$  has no boundary it is therefore unbounded.

Now fix  $\lambda \in L$ . As  $\eta(H \times \{\lambda\})$  is unbounded and path-connected, there exist points with arbitrary 2-norm modulo  $2\pi$  in  $\eta(H \times \{\lambda\})$ ; namely, there exists a point  $\mathbf{h}_0 \in H$  such that (mapped under  $\eta$ ):

$$\theta_{i,p}^{(i)} \equiv 0 \pmod{2\pi}. \tag{91}$$

This corresponds to  $n$  trivial measurements in the translation task—fixing the measurement outcomes to all be +1—followed by  $n$  operations that stabilize the initial state, leaving it unchanged. Note that  $\lambda$  is the image of  $\mathbf{h}_0$  under  $\Pi_L \circ \mathcal{F}$ . Assuming the model performs the translation task correctly, this fixes the measurement outcomes of the first  $n$  measurements to all be +1 for *all* points mapping to  $\lambda$  under  $\Pi_L \circ \mathcal{F}$ , as the next  $n$  outputs are just recapitulations of these first  $n$  measurement outcomes and they must be consistent for all inputs mapping to  $\lambda$ .

Thus, there exists some coordinate  $\theta_* = \theta_v^{(i)}$  such that, for any sufficiently large  $\theta_*$ , there exists a point in  $K$  with this  $\theta_*$  that maps to  $\lambda$ . Furthermore, the 2-norm of the inputs can be assumed to map to 1 under the bump function  $t$  by varying one of the other unbounded coordinates on  $\eta(H \times \{\lambda\})$ . Thus, there exist  $\mathbf{h}', \mathbf{h}'' \in U$  mapping to  $\lambda$  that describe qumode  $k$ -uniform weighted hypergraph states with some respective hyperedges  $e'_v, e''_v$  differing by 1.

By Lemma C.2, we have that there exists a measurement sequence (describable by the translation task) of length  $n - k + 2$  that antidistinguishes these three associated states with certainty. By then performing this antidistinguishing measurement sequence, the output for one of these  $\mathbf{h}_0, \mathbf{h}', \mathbf{h}''$  must then be incorrect. Thus, the model must obtain an infinite backward empirical cross entropy on these three sequences when followed by the antidistinguishing measurement sequence.  $\square$

## C.4 Expressivity Separation for Encoder-Decoder Models

Though autoregressive sequence models are perhaps conceptually the simplest as they directly map input tokens to output tokens, in practice encoder-decoder models outperform them (Sutskever et al., 2014; Vaswani et al., 2017). We now show that no encoder-decoder model (with similar technical assumptions as the autoregressive separation) can perform the introduced tasks to finite backward empirical cross entropy. The proofs will be similar to that of Theorems C.3 and C.4; however, as encoder-decoder models can see the entire input sequence at once, we do not directly have the freedom to choose the antidistinguishing measurement sequence as in the proofs of those theorems. This will change the details of the proofs here.

We consider an encoder-decoder model with structure given by Figure 1(b). The encoder of such a model is a function:

$$\mathcal{E}^r : (\mathbb{R}^m)^\ell \rightarrow L \tag{92}$$

where, as in the proofs of Theorem C.3 and C.4,  $\mathbf{r}$  is a random vector such that, for any  $\mathbf{r}$ ,  $\mathcal{E}^{\mathbf{r}}$  is deterministic. For the reasons discussed in Appendix C.3 we will take the  $\mathbf{r}$ -dependence to be implicit WLOG. We once again assume that  $L$  is a  $C^2$  contractible Finsler manifold.

As  $\mathcal{E}$  is a function of the *entire* input sequence rather than just the first  $n$  (or  $2n$ , in the case of the qumode separation), we have to appropriately modify our assumptions on its derivatives. We once again assume the existence of a contractible,  $(\dim(L) + 2)$ -dimensional, open subset  $U \subseteq K$ , where  $K$  once again is a subspace of inputs corresponding to the measurement of hypergraph state stabilizers. To match the full sequence length, though, we now have to assume that for  $\mathcal{E}$  on  $U \times \{\mathbf{v}\}$ —not just  $U$ , as in the autoregressive model separation—for all but isolated  $\mathbf{v} \in \mathbb{R}^{\ell - \dim(K)}$ ,  $\mathcal{E}$  is a strong submersion, and no sequence with limit point in  $\partial U \times \{\mathbf{v}\} \not\subseteq U \times \{\mathbf{v}\}$  maps to a sequence with limit point in  $L$  under  $\mathcal{E}$ .

#### C.4.1 Qubit Separation

With the preliminaries in place, we now prove our expressivity separation on the qubit-based task.

**Theorem C.5** (Encoder-decoder qubit hypergraph stabilizer measurement translation memory lower bound). *Consider an encoder-decoder model with  $C^2$  contractible Finsler latent manifold  $L$ , and encoder function*

$$\mathcal{E} : \mathbb{R}^{m(2n-k+3)} \rightarrow L. \quad (93)$$

Let  $V \subseteq \mathbb{R}^{m(n-k+3)}$  be  $\mathbb{R}^{m(n-k+3)}$  potentially with isolated points removed. Assume there exists a contractible, open subset  $U \subset K$ , where  $U$  is a  $C^1$  manifold of dimension at least  $\dim(L) + 2$  (where  $K \subset \mathbb{R}^{mn}$  is as described in equation (95)) such that for all  $\mathbf{v} \in V$ , on  $U \times \{\mathbf{v}\}$ ,  $\mathcal{E}$  is  $C^2$  and a strong submersion. Finally, assume no sequence with limit point in  $\partial U \times \{\mathbf{v}\} \not\subseteq U \times \{\mathbf{v}\}$  maps to a sequence with limit point in  $L$  under  $\mathcal{E}$ .

*This model cannot achieve a finite backward empirical cross entropy on the qubit  $(2n - k + 3, n, k)$ -hypergraph stabilizer measurement translation (without repetition) task due to quantum contextuality.*

*Proof.* Let

$$m = n \left( 1 + \binom{n-1}{k-1} \right) + \binom{n}{k} \quad (94)$$

be the dimension of each row of an input sentence to the model. Consider

$$R \equiv K \times (\mathbb{R}^m)^{n-k+3} \subset (\mathbb{R}^m)^n \times (\mathbb{R}^m)^{n-k+3} \cong (\mathbb{R}^m)^{2n-k+3} \quad (95)$$

with elements  $(\mathbf{Q}, \mathbf{P})$  of the following form:

1.  $\mathbf{Q} \in K$  is as in equation (79);
2.  $\mathbf{P} \in (\mathbb{R}^m)^{n-k+3}$  is an  $(n - k + 3) \times m$  matrix that is arbitrary.

Just as in the proof of Theorem C.3, it is obvious from this construction that  $K$  is an  $\binom{n}{k}$ -dimensional embedding of representations of  $k$ -uniform hypergraphs via their adjacency tensors. Thus, the states described by the measurement scenarios of nontrivial points in  $K$  are exactly qubit  $k$ -uniform weighted hypergraph states with, depending on the measurement results, perhaps overall phases on the stabilizers.

We will proceed as follows. First, we will show that when  $\dim(L)$  is sufficiently small,  $\mathcal{E}$  must map three distinct qubit  $k$ -uniform hypergraph states described by different  $\mathbf{Q}$  to the same point in latent space when  $\mathbf{P} = \mathbf{v}_0$ . Then, we will use Lemma C.1 to show that the stabilizers of these states give rise to an antidistinguishing measurement sequence of length  $n - k + 2$  once the phases on their stabilizers have been fixed to be identical. Finally, we will show that one can find  $\mathbf{P} \neq \mathbf{v}_0$  mapping to the same point in latent space that contains this antidistinguishing measurement sequence, forcing an incorrect measurement outcome on one of these states. This implies that there is an infinite backward empirical cross entropy on any finite set containing these three measurement sequences.

Let us begin by showing that  $\mathcal{E}|_R$  (i.e., the locally Lipschitz map that is  $\mathcal{E}$  restricted to  $R$ ) must map three nontrivially distinct  $\mathbf{Q}$  to the same point in latent space when  $\dim(L)$  is sufficiently small. We will achieve this by considering the restriction  $\mathcal{E}|_K$ , which is the (locally Lipschitz) restriction of  $\mathcal{E}$  to points of the form  $(\mathbf{Q}, \mathbf{v}_0) \in R$ . We will show that this map is not injective for small enough  $\dim(L)$ . As  $\mathcal{E}|_R$  lifts to  $\mathcal{E}|_K$ , this will show that three distinct  $\mathbf{Q}$  map to the same point in latent space under  $\mathcal{E}|_R$ . This is similar to the construction for  $\mathcal{F}|_K$  in the proof of Theorem C.3; we repeat it here for completeness.

By Theorem 5.2 of Rabier (1997), following our assumptions,  $\mathcal{E}|_{U \times \{\mathbf{v}\}}$  is a fiber bundle for all  $\mathbf{v} \in V$  with base space  $C^1$ -diffeomorphic to  $L$ , and induces a  $C^1$ -diffeomorphism  $\eta_{\mathbf{v}} : H_{\mathbf{v}} \times L \rightarrow U \times \{\mathbf{v}\}$ :

$$H_{\mathbf{v}} \times L \cong U \times \{\mathbf{v}\}; \quad (96)$$

in particular,  $\Pi_L \circ \mathcal{E}|_{U \times \{\mathbf{v}\}}$  is a trivial bundle, and  $H_{\mathbf{v}}$  is thus path-connected and of dimension:

$$\dim(H_{\mathbf{v}}) = \dim(U) - \dim(L) \geq 2. \quad (97)$$

By the transitivity of  $C^1$ -diffeomorphisms, all  $H_{\mathbf{v}}$  are  $C^1$ -diffeomorphisms and can be taken to be some  $H$  WLOG. We thus have the trivial bundle structure:

$$H \times L \times V \cong U \times V, \quad (98)$$

with fibers  $C^1$ -diffeomorphic to  $H \times V$  and base space  $C^1$ -diffeomorphic to  $L$ . We claim that  $\eta_{\mathbf{v}_0}(H \times \{\lambda\} \times \{\mathbf{v}_0\})$  is unbounded for all  $\lambda \in L, \mathbf{v}_0 \in V$ . To see this, first note that as  $\eta_{\mathbf{v}_0}$  is a homeomorphism, the boundary of  $\eta_{\mathbf{v}_0}(H \times \{\lambda\} \times \{\mathbf{v}_0\})$  for all  $\lambda \in L$  must be a subset of  $\partial U \times \{\mathbf{v}_0\}$  for all  $\mathbf{v}_0 \in V$ . Assume now that it is nonempty, i.e., that there existed a Cauchy sequence with limit point in  $\partial H \times \{\lambda\} \times \{\mathbf{v}_0\}$  that mapped to a Cauchy sequence with limit point in  $\partial U \times \{\mathbf{v}_0\}$  under  $\eta_{\mathbf{v}_0}$ . Then, a sequence with limit point in  $\partial U \times \{\mathbf{v}_0\}$  would have base point  $\lambda \in L$ , violating our assumption that no sequence with limit point in the boundary of  $U \times \{\mathbf{v}_0\}$  has limit point in  $L$  under  $\mathcal{E}$ . Thus,  $\eta_{\mathbf{v}_0}(H \times \{\lambda\} \times \{\mathbf{v}_0\})$  has no boundary. In particular, as  $\eta_{\mathbf{v}_0}(H \times \{\lambda\} \times \{\mathbf{v}_0\})$  is contractible, it is not compact as closed manifolds cannot be contractible. As  $\eta_{\mathbf{v}_0}(H \times \{\lambda\} \times \{\mathbf{v}_0\}) \subset K \times \{\mathbf{v}_0\}$  has no boundary it is therefore unbounded.

Now fix  $\lambda \in L, \mathbf{v}_0 \in V$ . As  $\eta_{\mathbf{v}_0}(H \times \{\lambda\} \times \{\mathbf{v}_0\})$  is unbounded and path-connected, there exist points with arbitrary 2-norm modulo  $2\pi$  in  $\eta_{\mathbf{v}_0}(H \times \{\lambda\} \times \{\mathbf{v}_0\})$ ; namely, there exists a point  $(\mathbf{h}_0, \mathbf{v}_0) \in H \times \{\mathbf{v}_0\}$  such that (mapped under  $\eta$ ):

$$\theta_{i,X}^{(i)} \equiv 0 \pmod{2\pi}. \quad (99)$$

This corresponds to trivial measurements in the translation task, fixing the measurement outcomes to all be +1. Note that  $\lambda$  is the image of  $(\mathbf{h}_0, \mathbf{v}_0)$  under  $\mathcal{E}$ . Assuming the model performs the translation task correctly, this fixes the measurement outcomes of the first  $n$  measurements to all be +1 for *all* points mapping to  $\lambda$  under  $\mathcal{E}$  as the decoder  $\mathcal{D}$  only depends on  $\lambda$ .

Thus, there exists some coordinate  $\theta_* = \theta_{\frac{i}{v}}^{(i)}$  such that, for any sufficiently large  $\theta_*$ , there exists a point in  $K \times \{\mathbf{v}_0\}$  with this  $\theta_*$  that maps to  $\lambda$ . Furthermore, as  $H$  is of dimension at least 2, the 2-norm of the inputs can be assumed to be nonzero modulo  $2\pi$  by varying one of the other coordinates on  $\eta_{\mathbf{v}_0}(H \times \{\lambda\} \times \{\mathbf{v}_0\})$ . Thus, there exist  $(\mathbf{h}', \mathbf{v}_0), (\mathbf{h}'', \mathbf{v}_0) \in U \times \{\mathbf{v}_0\}$  mapping to  $\lambda$  that describe qubit  $k$ -uniform weighted hypergraph states with some respective hyperedges  $e'_{\frac{i}{v}}, e''_{\frac{i}{v}}$  differing by 1.

By Lemma C.1, we have that there exists a measurement sequence (describable by the translation task) of length  $n - k + 2$  that antidistinguishes these three associated states with certainty. As  $V$  is  $\mathbb{R}^{m(n-k+3)}$  up to potentially the removal of isolated points, by varying the final coordinate—corresponding to measurements *after* the first  $n - k + 2$  measurements—any given antidistinguishing measurement of length  $n - k + 2$  can be assumed to be in  $V$ . As the construction given in equation (98) is unchanged when taking  $\eta_{\mathbf{v}}$  rather than  $\eta_{\mathbf{v}_0}$  as described, we can take  $\mathbf{v}$  to be this antidistinguishing measurement sequence while still ensuring the associated three states map to the same point in the latent space of the model. Therefore, the output for one of these  $\mathbf{h}_0, \mathbf{h}', \mathbf{h}''$  must then be incorrect. Thus, the model must obtain an infinite backward empirical cross entropy on these three sequences when followed by the antidistinguishing measurement sequence.  $\square$

### C.4.2 Qumode Separation

The separation for the qumode version of the hypergraph stabilizer measurement task proceeds similarly. For technical reasons, in the proof for the qumode separation we require the use of the ‘‘bubble wrap’’ function we define in equation (85).

**Theorem C.6** (Encoder-decoder qumode hypergraph stabilizer measurement translation memory lower bound). *Consider an encoder-decoder model with  $C^2$  contractible Finsler latent manifold  $L$ , and encoder function*

$$\mathcal{E} : \mathbb{R}^{m(3n-k+3)} \rightarrow L \times \mathbb{R}^n. \quad (100)$$

*Let  $V \subseteq \mathbb{R}^{m(n-k+3)}$  be  $\mathbb{R}^{m(n-k+3)}$  potentially with isolated points removed. Assume there exists a contractible, open subset  $U \subset K$ , where  $U$  is a  $C^1$  manifold of dimension at least  $\dim(L) + 2$  (where  $K \subset \mathbb{R}^{2mn}$  is as described in equation (102)) such that for all  $\mathbf{v} \in V$ , on  $U \times \{\mathbf{v}\}$ ,  $\mathcal{E}$  onto  $L$  is  $C^2$  and a strong submersion. Finally, assume no sequence with limit point in  $\partial U \times \{\mathbf{v}\} \not\subset U \times \{\mathbf{v}\}$  maps to a sequence with limit point in  $L$  under  $\mathcal{E}$ .*

*This model cannot achieve a finite backward empirical cross entropy on the qumode  $(3n - k + 3, n, k)$ -hypergraph stabilizer measurement translation (without repetition) task due to quantum contextuality.*

*Proof.* Let

$$m = n \left( 2 + \binom{n-1}{k-1} \right) \quad (101)$$

be the dimension of each row of an input sentence to the model. Consider

$$R \equiv K \times (\mathbb{R}^m)^{n-k+3} \subset (\mathbb{R}^m)^{2n} \times (\mathbb{R}^m)^{n-k+3} \cong (\mathbb{R}^m)^{3n-k+3} \quad (102)$$

with elements  $(\mathbf{Q}, \mathbf{P})$  of the following form:

1.  $\mathbf{Q} \in K$  is as in equation (88);
2.  $\mathbf{P} \in (\mathbb{R}^m)^{n-k+3}$  is an  $(n - k + 3) \times m$  matrix that is arbitrary.

Just as in the proof of Theorem C.4, it is obvious from this construction that  $K$  is an  $\binom{n}{k}$ -dimensional embedding of representations of  $k$ -uniform hypergraphs via their adjacency tensors. Thus, the states described by the measurement scenarios of nontrivial points in  $K$  are exactly qumode  $k$ -uniform weighted hypergraph states with, depending on the measurement results, perhaps overall phases on the stabilizers.

We will proceed as follows. First, we will show that when  $\dim(L)$  is sufficiently small,  $\mathcal{E}$  must map three distinct qumode  $k$ -uniform hypergraph states described by different  $\mathbf{Q}$  to the same point in latent space when  $\mathbf{P} = \mathbf{v}_0$ . Then, we will use Lemma C.2 to show that the stabilizers of these states give rise to an antidistinguishing measurement sequence of length  $n - k + 2$  once the phases on their stabilizers have been fixed to be identical. Finally, we will show that one can find  $\mathbf{P} \neq \mathbf{v}_0$  mapping to the same point in latent space that contains this antidistinguishing measurement sequence, forcing an incorrect measurement outcome on one of these states. This implies that there is an infinite backward empirical cross entropy on any finite set containing these three measurement sequences.

Let us begin by showing that  $\mathcal{E}|_R$  (i.e., the locally Lipschitz map that is  $\mathcal{E}$  restricted to  $R$ ) must map three nontrivially distinct  $\mathbf{Q}$  to the same point in latent space when  $\dim(L)$  is sufficiently small. We will achieve this by considering the restriction  $\mathcal{E}|_K$ , which is the (locally Lipschitz) restriction of  $\mathcal{E}$  to points of the form  $(\mathbf{Q}, \mathbf{v}_0) \in R$ . We will show that this map is not injective for small enough  $\dim(L)$ . As  $\mathcal{E}|_R$  lifts to  $\mathcal{E}|_K$ , this will show that three distinct  $\mathbf{Q}$  map to the same point in latent space under  $\mathcal{E}|_R$ . This is similar to the construction for  $\mathcal{F}|_K$  in the proof of Theorem C.4; we repeat it here for completeness.

By Theorem 5.2 of Rabier (1997), following our assumptions,  $\mathcal{E}|_{U \times \{\mathbf{v}\}}$  is a fiber bundle for all  $\mathbf{v} \in V$  with base space  $C^1$ -diffeomorphic to  $L$ , and induces a  $C^1$ -diffeomorphism  $\eta_{\mathbf{v}} : H_{\mathbf{v}} \times L \rightarrow U \times \{\mathbf{v}\}$ :

$$H_{\mathbf{v}} \times L \cong U \times \{\mathbf{v}\}; \quad (103)$$

in particular,  $\Pi_L \circ \mathcal{E}|_{U \times \{\mathbf{v}\}}$  is a trivial bundle, and  $H_{\mathbf{v}}$  is thus path-connected and of dimension:

$$\dim(H_{\mathbf{v}}) = \dim(U) - \dim(L) \geq 2. \quad (104)$$

By the transitivity of  $C^1$ -diffeomorphisms, all  $H_{\mathbf{v}}$  are  $C^1$ -diffeomorphisms and can be taken to be some  $H$  WLOG. We thus have the trivial bundle structure:

$$H \times L \times V \cong U \times V, \quad (105)$$

with fibers  $C^1$ -diffeomorphic to  $H \times V$  and base space  $C^1$ -diffeomorphic to  $L$ . We claim that  $\eta_{\mathbf{v}_0}(H \times \{\lambda\} \times \{\mathbf{v}_0\})$  is unbounded for all  $\lambda \in L, \mathbf{v}_0 \in V$ . To see this, first note that as  $\eta_{\mathbf{v}_0}$  is a homeomorphism, the boundary of  $\eta_{\mathbf{v}_0}(H \times \{\lambda\} \times \{\mathbf{v}_0\})$  for all  $\lambda \in L$  must be a subset of  $\partial U \times \{\mathbf{v}_0\}$  for all  $\mathbf{v}_0 \in V$ . Assume now that it is nonempty, i.e., that there existed a Cauchy sequence with limit point in  $\partial H \times \{\lambda\} \times \{\mathbf{v}_0\}$  that mapped to a Cauchy sequence with limit point in  $\partial U \times \{\mathbf{v}_0\}$  under  $\eta_{\mathbf{v}_0}$ . Then, a sequence with limit point in  $\partial U \times \{\mathbf{v}_0\}$  would have base point  $\lambda \in L$ , violating our assumption that no sequence with limit point in the boundary of  $U \times \{\mathbf{v}_0\}$  has limit point in  $L$  under  $\mathcal{E}$ . Thus,  $\eta_{\mathbf{v}_0}(H \times \{\lambda\} \times \{\mathbf{v}_0\})$  has no boundary. In particular, as  $\eta_{\mathbf{v}_0}(H \times \{\lambda\} \times \{\mathbf{v}_0\})$  is contractible, it is not compact as closed manifolds cannot be contractible. As  $\eta_{\mathbf{v}_0}(H \times \{\lambda\} \times \{\mathbf{v}_0\}) \subset K \times \{\mathbf{v}_0\}$  has no boundary it is therefore unbounded.

Now fix  $\lambda \in L, \mathbf{v}_0 \in V$ . As  $\eta_{\mathbf{v}_0}(H \times \{\lambda\} \times \{\mathbf{v}_0\})$  is unbounded and path-connected, there exist points with arbitrary 2-norm modulo  $2\pi$  in  $\eta_{\mathbf{v}_0}(H \times \{\lambda\} \times \{\mathbf{v}_0\})$ ; namely, there exists a point  $(\mathbf{h}_0, \mathbf{v}_0) \in H \times \{\mathbf{v}_0\}$  such that (mapped under  $\eta$ ):

$$\theta_{i,p}^{(i)} \equiv 0 \pmod{2\pi}. \quad (106)$$

This corresponds to  $n$  trivial measurements in the translation task—fixing the measurement outcomes to all be +1—followed by  $n$  operations that stabilize the initial state, leaving it unchanged. Note that  $\lambda$  is the image of  $(\mathbf{h}_0, \mathbf{v}_0)$  under  $\mathcal{E}$ . Assuming the model performs the translation task correctly, this fixes the measurement outcomes of the first  $n$  measurements to all be +1 for *all* points mapping to  $\lambda$  under  $\mathcal{E}$  as the decoder  $\mathcal{D}$  only depends on  $\lambda$ .

Thus, there exists some coordinate  $\theta_* = \theta_v^{(i)}$  such that, for any sufficiently large  $\theta_*$ , there exists a point in  $K \times \{\mathbf{v}_0\}$  with this  $\theta_*$  that maps to  $\lambda$ . Furthermore, as  $H$  is of dimension at least 2, the 2-norm of the inputs can be assumed to be nonzero modulo  $2\pi$  by varying one of the other coordinates on  $\eta_{\mathbf{v}_0}(H \times \{\lambda\} \times \{\mathbf{v}_0\})$ . Thus, there exist  $(\mathbf{h}', \mathbf{v}_0), (\mathbf{h}'', \mathbf{v}_0) \in U \times \{\mathbf{v}_0\}$  mapping to  $\lambda$  that describe qumode  $k$ -uniform weighted hypergraph states with some respective hyperedges  $e'_v, e''_v$  differing by 1.

By Lemma C.2, we have that there exists a measurement sequence (describable by the translation task) of length  $n - k + 2$  that antidistinguishes these three associated states with certainty. As  $V$  is  $\mathbb{R}^{m(n-k+3)}$  up to potentially the removal of isolated points, by varying the final coordinate—corresponding to measurements *after* the first  $n - k + 2$  measurements—any given antidistinguishing measurement of length  $n - k + 2$  can be assumed to be in  $V$ . As the construction given in equation (105) is unchanged when taking  $\eta_{\mathbf{v}}$  rather than  $\eta_{\mathbf{v}_0}$  as described, we can take  $\mathbf{v}$  to be this antidistinguishing measurement sequence while still ensuring the associated three states map to the same point in the latent space of the model. Therefore, the output for one of these  $\mathbf{h}_0, \mathbf{h}', \mathbf{h}''$  must then be incorrect. Thus, the model must obtain an infinite backward empirical cross entropy on these three sequences when followed by the antidistinguishing measurement sequence.  $\square$

## D CV $k$ -HRNNs as a Quantization of RNNs

The construction of CV  $k$ -HRNNs described in Section 3 is the quantization of alternating the classical Hamiltonian dynamics under the Hamiltonians:

$$G = \sum_{\substack{b \in \mathcal{N} \\ \bar{i} \in C_{\mathcal{M}, k-1}}} \phi_{b, \bar{i}} q_{\bar{i}} \otimes p_b, \quad (107)$$

$$H = \sum_{c \in \mathcal{O}} p_c \otimes \left( \sum_{b \in \mathcal{N}} \gamma_{c,b} p_b + \sum_{\bar{j} \in C_{\mathcal{N}, k-1}} \theta_{c, \bar{j}} q_{\bar{j}} \right). \quad (108)$$



Consider now discrete time dynamics under this alternating Hamiltonian evolution with fresh ancilla qubits indexed by  $\mathcal{M}, \mathcal{O}$  supplied at each time step, where  $p_c, q_c = 0$  for all  $c \in \mathcal{O}$ . Furthermore, assume the dynamics begin with  $p_b = 0$  for all  $b \in \mathcal{N}$ . After evolution by  $G$  followed by  $H$ , we have the new canonical variables (given by primed notation) for  $a \in \mathcal{M}, b \in \mathcal{N}, c \in \mathcal{O}$ :

$$\begin{aligned} p'_b &= p_b = 0, \\ q'_b &= q_b + \sum_{\bar{i} \in C_{\mathcal{M},k}} \phi_{b,\bar{i}} q_{\bar{i}}, \\ q'_c &= \sum_{b \in \mathcal{N}} \gamma_{c,b} p'_b + \sum_{\bar{j} \in C_{\mathcal{N},k-1}} \theta_{c,\bar{j}} q'_{\bar{j}} = \sum_{\bar{j} \in C_{\mathcal{N},k-1}} \theta_{c,\bar{j}} q'_{\bar{j}}. \end{aligned} \tag{109}$$

In particular, a classical RNN obeying these alternating Hamiltonian dynamics updates its latent vector as:

$$\boldsymbol{\lambda}' = \boldsymbol{\lambda} + \mathbf{f}_{k-1}(\mathbf{x}), \tag{110}$$

where  $\mathbf{x}$  is the current input to the RNN and  $\mathbf{f}_{k-1}$  is an arbitrary degree- $(k-1)$  polynomial in the entries of  $\mathbf{x}$ . Similarly, it outputs:

$$\mathbf{y} = \mathbf{g}_{k-1}(\boldsymbol{\lambda}'), \tag{111}$$

where  $\mathbf{g}_{k-1}$  is an arbitrary degree- $(k-1)$  polynomial in the entries of  $\boldsymbol{\lambda}'$ . For sufficiently large  $k$ , HRNNs can then be thought of as quantizations of RNNs with updates:

$$\boldsymbol{\lambda}' = \boldsymbol{\lambda} + \mathbf{f}(\mathbf{x}), \tag{112}$$

$$\mathbf{y} = \mathbf{g}(\boldsymbol{\lambda}'), \tag{113}$$

for analytic functions  $\mathbf{f}, \mathbf{g}$ .

## E Time Complexity

### E.1 Optimal Classical Algorithms

Our achieved memory separation is asymptotically optimal by the results of Somma et al. (2006), which gives an  $O(n^k)$ -memory classical simulation algorithm for the quantum model we consider. This is accomplished via efficient representations of the dynamical Lie algebra of the model which is of dimension  $\Theta(n^k)$ . As this algorithm requires multiplications of  $\Theta(n^k)$ -dimensional representations of members of this algebra, it achieves a time complexity of  $O(n^{\omega k})$  per unit cell of the  $k$ -HRNN, where  $\omega \geq 2$  is the matrix multiplication exponent (currently known to be at most 2.37187 (Duan et al., 2022), but for reasonable  $n$  no better than  $\log_2(7) \approx 2.8$  using Strassen’s algorithm (Strassen, 1969)). For  $k = 2$  it is further known that  $O(n^2)$ -time classical simulation algorithms exist for a unit cell of a  $k$ -HRNN (Aaronson & Gottesman, 2004; Calcluth et al., 2022). As mentioned in Section 3 and Appendix B.1, each unit cell of a  $k$ -HRNN is in  $\text{QNC}_{\text{wf}}^0$ , i.e., can be implemented in constant depth on a quantum computer assuming access to quantum fan-out (or logarithmic depth if not) (Moore & Nilsson, 2001; 1998; Høyer & Špalek, 2005).

Though our quantum model achieves time separations over the best-known classical simulations of the model, it is important here to reemphasize that our proved separation is a *memory* (or *communication*) separation rather than a *time* separation. Though our memory lower-bound gives a “sequential” time complexity (i.e., circuit *size*) lower-bound for any classical model performing this task, in principle there could exist a “parallelized” classical algorithm which is time efficient (i.e., have short circuit *depth*). Indeed, this is the case for our quantum model: though each unit cell is in  $\text{QNC}_{\text{wf}}^0$ , which  $\text{QNC}_{\text{wf}}^0$  operation is applied depends on (i.e., is controlled by) the  $\sim n^{k-1}$ -dimensional input token  $\mathbf{x}_i$ .

Trivially, no classical autoregressive model with unit cells composed of constant-depth circuits with fan-out—i.e.,  $\text{NC}^0$  circuits—can perform this task as classically such circuits can only read a constant number of inputs. However, this does not discount the possibility that an autoregressive classical model composed

of logarithmic-depth classical circuits, i.e., with unit cells in  $\text{NC}^1$ , could perform this task (albeit still with a communication complexity of  $\Omega(n^k)$  by our lower-bound). Though this seems unlikely, we now give an alternative, *online* (or *streamed*) formulation of the  $(\ell, k, n)$ -HSMT task where the tokens are of constant dimension and are streamed; this is a common model of sequence learning extremely long sequences (Domingos & Hulten, 2000; Gaber et al., 2005; Gama, 2012). In this setting, the complexity (i.e., circuit size) per unit cell of the model is fixed by the stream rate and thus the memory requirements of the model is the quantity of interest to be optimized, as in our proof.

## E.2 Online $(\ell, n, k)$ -HSMT

Given an instance of the  $(\ell, n, k)$ -HSMT task, we define its associated  $(\ell, n, k)$ -*online HSMT* ( $(\ell, n, k)$ -OHSMT) task in the following way. Let

$$\mathbf{x} = (\mathbf{x}_1, \dots, \mathbf{x}_\ell)^\top \quad (114)$$

be the sequence of input tokens associated with the  $(\ell, n, k)$ -HSMT task as described in Section 4.1 or Appendix B.2. Note that

$$\dim(\mathbf{x}_i) \equiv m = O(n^{k-1}). \quad (115)$$

The associated  $(\ell, n, k)$ -OHSMT instead has *amortized inputs*:

$$\tilde{\mathbf{x}} = \begin{pmatrix} x_{1,1} & 0 \\ \vdots & \vdots \\ x_{1,m-1} & 0 \\ x_{1,m} & 1 \\ x_{2,1} & 0 \\ \vdots & \vdots \\ x_{\ell,m} & 1 \end{pmatrix}, \quad (116)$$

where each row  $(x_{i,j}, a_{i,j})$  is now in  $\mathbb{R}^2$ . Here,  $a_{i,j}$  is one if and only if  $j = m$ . The  $k$ -HRNNs described in Section 3 or Appendix B.1 can still perform this task with the addition of a single ancilla qumode or qubit, respectively, by passing what was the “output register” (labeled  $|GKP\rangle$  in Figure 2) to future cells, and only performing a final measurement in the  $X$  or  $\hat{p}$  basis when  $a_{i,j} = 1$ .

Effectively, this construction trades off the dimension of the input token for the length of the sequence in the translation task. As now the circuit size per unit cell is a constant, the  $(\ell, n, k)$ -OHSMT task can then be viewed naturally as an online sequence learning problem where the tokens are continually streamed to the model from an environment at some fixed rate (Domingos & Hulten, 2000; Gaber et al., 2005; Gama, 2012). As the time between tokens in the streaming model is some fixed constant, the resource to be optimized for is the memory required by the model performing the learning task; this is the resource for which we have proved our quantum-classical separations.

## E.3 Hybrid Quantum-Classical Training

$k$ -HRNN are efficiently trainable as their associated dynamical Lie algebra dimensions grow as  $\binom{n}{k} \sim n^k$ . As discussed in Section 2.3, this suggests training times on the order of poly( $n^k$ ) per training iteration to even resolve the gradients of the model (Larocca et al., 2022a; Rudolph et al., 2023; Fontana et al., 2023; Ragone et al., 2023). As previously discussed in Appendix E.1, there exists an  $\Theta(n^k)$ -memory classical algorithm capable of simulating  $k$ -HRNNs (Somma et al., 2006). Though not time-optimal—the algorithm takes time  $\sim n^{2.8k}$  (for reasonable  $n$ ) per gate of the  $k$ -HRNN—there is the possibility that there exists an  $\sim n^k$ -time classical algorithm which simulates a  $k$ -HRNN unit cell. What implications does this loophole have on our separation?

If such a simulation algorithm were found, one could classically *train* a  $k$ -HRNN as efficiently as one could on a quantum computer, but still leverage a resource advantage by using a quantum computer at time of

inference. Interestingly, in this scenario one can consider the  $k$ -HRNN as a “quantum compression” of a quantum-inspired classical neural network model: at training time, one implements classically a simulation of a  $k$ -HRNN, where the classical memory used by the simulation is  $N$ . Once training is finished, one implements the model on a quantum computer using  $\sim N^{\frac{1}{k}}$  qubits or qumodes. All future evaluations of the model now use polynomially fewer resources than the classical implementation, with the degree of separation depending on  $k$ . This also opens the possibility for the quantum model to “take over” training when in the vicinity of a minimum, where the loss landscape is believed to be more amenable for training on a quantum device (Anschuetz, 2022; Anschuetz & Kiani, 2022). We leave further investigation of the implications of hybrid quantum-classical training algorithms for future work.